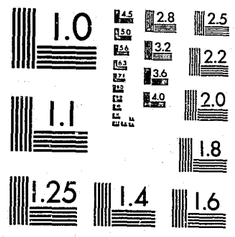

U.S. Department of Justice
National Institute of Justice

NIJ

Technology Assessment Program

Police Handgun Ammunition: Incapacitation Effects Volume I: Evaluation

NIJ Report 100-83

a publication of the **National Institute of Justice**

ABOUT THE TECHNOLOGY ASSESSMENT PROGRAM

The Technology Assessment Program is sponsored by the Office of Development, Testing, and Dissemination of the National Institute of Justice (NIJ), U.S. Department of Justice. The program responds to the mandate of the Justice System Improvement Act of 1979, which created NIJ and directed it to encourage research and development to improve the criminal justice system and to disseminate the results to Federal, State, and local agencies.

The Technology Assessment Program is an applied research effort that determines the technological needs of justice system agencies, sets minimum performance standards for specific devices, tests commercially available equipment against those standards, and disseminates the standards and the test results to criminal justice agencies nationwide and internationally.

The program operates through:

The *Technology Assessment Program Advisory Council* (TAPAC) consisting of nationally recognized criminal justice practitioners from Federal, State, and local agencies, which assesses technological needs and sets priorities for research programs and items to be evaluated and tested.

The *Law Enforcement Standards Laboratory* (LESL) at the National Bureau of Standards, which develops voluntary national performance standards for compliance testing to ensure that individual items of equipment are suitable for use by criminal justice agencies. The standards are based upon laboratory testing and evaluation of representative samples of each item of equipment to determine the key attributes, develop test methods, and establish minimum performance requirements for each essential attribute. In addition to the highly technical standards, LESL also produces user guides that explain in nontechnical terms the capabilities of available equipment.

The *Technology Assessment Program Information Center* (TAPIC) operated by the International Association of Chiefs of Police (IACP), which supervises a national compliance testing program conducted by independent agencies. The standards developed by LESL serve as performance benchmarks against which commercial equipment is measured. The facilities, personnel, and testing capabilities of the independent laboratories are evaluated by LESL prior to testing each item of equipment, and LESL helps the Information Center staff review and analyze data. Test results are published in Consumer Product Reports designed to help justice system procurement officials make informed purchasing decisions.

All publications issued by the National Institute of Justice, including those of the Technology Assessment Program, are available from the National Criminal Justice Reference Service (NCJRS), which serves as a central information and reference source for the Nation's criminal justice community. For further information, or to register with NCJRS, write to the National Institute of Justice, National Criminal Justice Reference Service, Washington, DC 20531.

James K. Stewart, Director
National Institute of Justice

For sale by the Superintendent of Documents, U.S. Government Printing Office, Washington, D.C. 20402

Technology Assessment Program

Police Handgun Ammunition: Incapacitation Effects Volume I: Evaluation

NIJ Report 100-83

William J. Bruchey, Jr.
Ballistic Research Laboratory
U.S. Army Armament Research and Development Command
Aberdeen Proving Ground, MD 21005

and

Daniel E. Frank
Law Enforcement Standards Laboratory
National Engineering Laboratory
National Bureau of Standards
Washington, DC 20234

Prepared by
Law Enforcement Standards Laboratory
National Engineering Laboratory
National Bureau of Standards
Washington, DC 20234

Prepared for
National Institute of Justice
U.S. Department of Justice
Washington, DC 20531

U.S. DEPARTMENT OF JUSTICE
National Institute of Justice

U.S. DEPARTMENT OF JUSTICE
National Institute of Justice
James K. Stewart
Director

Acknowledgments

This report was prepared by the Law Enforcement Standards Laboratory of the National Bureau of Standards under the direction of Ronald C. Dobbyn and Daniel E. Frank, successive Program Managers, and Lawrence K. Eliason, Chief of LESL. Special recognition is due to Lester D. Shubin, Program Manager, National Institute of Justice, whose foresight, faith, determination, and good counsel made this project possible.

Foreword

This report on Police Handgun Ammunition continues the tradition of the Technology Assessment Program, whose goal is to enable purchasers of criminal justice equipment to make informed purchasing decisions that consider both economy and effectiveness. Millions of dollars have been saved in purchases of communications equipment, special protective equipment, and other tools of the criminal justice system guided by performance standards established by the program.

Even more significant than the cost savings are the lives saved by the program. The lightweight armor now widely used by police was developed under the Technology Assessment Program. Since its introduction, the armor has saved the lives of more than 500 law enforcement officers.

The National Institute of Justice sponsored this study to provide the law enforcement community with criteria for deciding what ammunition is most suitable for their needs. Rarely is a law enforcement officer forced to fire his service revolver. However, in such situations, a person posing a life-endangering threat to an officer or to others must be effectively incapacitated. Under these extreme circumstances the police officer must have the most reliable ammunition available, yet the ammunition must not endanger the safety of bystanders. These are vital considerations law enforcement agencies must take into account in selecting handgun ammunition, and the data presented here proceed from these basic concerns.

We believe this report will help inform the administrative process of selecting the most cost-effective product. As police agencies continue to operate within budget constraints, the Technology Assessment Program will maintain its effort to be a source of practical and useful information that increases public safety while saving dollars.

James K. Stewart,
Director
National Institute of Justice

CONTENTS

EXECUTIVE SUMMARY

The objectives of this study were to examine theories prior to 1970 that have been used to rank bullet effectiveness, develop new methods and theories as appropriate, and to examine the ricochet potential/characteristics for handgun bullets. The kinetic energy theory of Hatcher and the energy deposit theory of the U.S. Army and Dr. DeMaio were examined and found to be lacking in one respect or another. A new measure of handgun bullet effectiveness against human targets was developed. The new measure is called the Relative Incapacitation Index (RII) and is explained in this report. A limited study of handgun bullet ricochet was undertaken, but definitive conclusions and recommendation were not reached. In general, all handgun bullets can ricochet and pose a danger to bystanders. The harder and the more solid the bullet, the more likely a dangerous ricochet can occur; but that does not necessarily mean one will.

Hatcher's Index considers only measurable parameters of the bullet. DeMaio's work is an improvement. It considers only the energy transferred to the target, again a measurable quantity, to be effective. The present work considers:

1. The ability of the average police officer to deliver effective fire.
2. The relative effectiveness of hits at different locations and depths of penetration into a human target.
3. Rapid incapacitation as the preferred effect independent of eventual death.
4. The performance of bullets in a reproducible target medium.
5. A method to extend the ranking system to variations in cartridge loadings without an extensive new test program.

The first issue examined was marksmanship. Statistical data on the performance of trained shooters tested under stress were located and analyzed.

Next, a computerized three-dimensional representation of the human torso developed by the U.S. Army was modified to incorporate measures of incapacitation. This "computerized man" is built of small volume segments, each segment of which was assigned a number between 0 and 10 by medical personnel. The number is representative of the relative importance of a particular location (tissue) within a person to incapacitation (stopping further aggression). A computer program or model was then generated that has the capability of "firing" at the "Computer Man" and tracing the trajectory of the hit completely through the volume of the target. A total of 10,000 shots were then "fired" at the Computer Man, to achieve a distribution of trajectories equivalent to that of the experimental shooter data. For each shot the Computer Man segments penetrated by the trajectory were identified and recorded. At the end of the simulated firing, the segment values at each 1-cm of depth of the Computer Man target were averaged (shots that missed the target were recorded as zero at all depths).

The set of numbers so created, which is a function of projectile penetration depth, represents the average vulnerability of the human body to incapacitation from projectiles fired by trained shooters under stress. We call these numbers the Vulnerability Index (V. Ind.) function.

The next issue examined was the performance of various bullets in a tissue simulant. The tissue simulant chosen for this study was ordnance gelatin. Ordnance gelatin was selected for the following reasons:

1. Similarity between bullet retardation in gelatin and animal tissue.
2. Similarity between the size and shape of the temporary cavity in gelatin and tissue.
3. Similarity between the permanent cavity remaining in tissue and gelatin after the passage of a bullet.
4. Homogeneity/reproducibility of the gelatin response to bullet penetration.
5. The material has been in use since the 1940's for wound ballistics experiments yielding a reasonable amount of historical data for comparisons.

Bullets were fired at blocks of ordnance gelatin. Since the physical stress introduced into a target material can be related to the maximum displacement of the material, the volume and shape of the maximum instantaneous cavity created by the penetration of the bullet was chosen as the performance measure of the interaction between the projectile and the gelatin. The volume of the cavity is weighted (multiplied) by the V. Ind. at each increment of depth to determine the RII of the projectile. *Specifically, the RII is defined as the product of the volume of the Maximum Temporary Cavity (MTC) produced by the interaction of a projectile and the tissue simulant (gelatin) at a given depth and the average vulnerability to incapacitation at that depth summed together for the entire penetration depth of the bullet to a maximum depth of 22 cm.* The 22-cm limit is a consequence of the fact that the V. Ind. is zero at depths greater than 22 cm.

To develop a simple methodology for predicting the RII for new cartridge loadings, the experimental RII vs. velocity data was analyzed. It was discovered that an exponential equation containing suitable constants combined with the bullet's striking velocity could adequately predict a bullet's performance. This enables an individual or agency to determine the RII of rounds not included in this report by simply measuring the velocity of a given bullet fired from the weapon with which it will be used, if the bullet configuration is such that the coefficients presented in this report are appropriate. The exact form of the predictive equation is presented in the body of this report. Appendix B provides a tabulation of the constants required to use the predictive equation.

A large number of different cartridges made by various manufacturers were fired from representative handguns. The data gathered were combined with the predictive equation and the cartridges ranked by RII. Table 1 arranges the tested cartridges by caliber, bullet weight, bullet construction, and manufacturer. Table 2 arranges the tested cartridges by RII within calibers and includes bullet weight, bullet construction, velocity, and manufacturer.

Finally, a word on how much RII is best. It is the opinion of the authors that RII's of less than 10 are representative of bullets that produce low-volume maximum temporary cavities; therefore, the probability of the MTC affecting vital tissue is low. It would then appear that the higher the RII the better. It was observed in this study that nondeforming bullets can achieve effective RII's if they have relatively high velocity. However, the same performance can be achieved with deforming bullets at low velocities. It is the observation of the authors that deforming projectiles with RII's 30 and below generally did not overpenetrate the target while giving reasonable size MTC's.

There is no ideal firearm system (weapon/ammunition) for all situations. Each law enforcement department must evaluate its own special requirements and choose a defensive weapon system capable of meeting its needs. However, this study has shown that for handguns in 9 mm/38 caliber to 45 caliber range, a deforming projectile, driven at a velocity above the minimum deformation velocity, and an RII between 10 and 30 is a reasonable goal for handgun ammunition for use against a normally dressed assailant in an urban environment.

*The use of brand, trade, or manufacturers' names in this document in no way constitutes endorsement of these products by the National Bureau of Standards or any other other agency of the Federal Government.

TABLE 1. *Predicted performance of commercially available handgun ammunition.*

Cartridge	Bullet weight (grains)	Bullet type	Manufacturer	Barrel length (in)	Velocity			Relative incapacitation index (RII)
					Nominal[b] (fps)	Measured (fps)	(mps)	
380 Auto	85	JHP(Silvertip)	Winchester	3.88	1000	986	300	13.4[a]
9 mm	100	FMJ	Smith+Wesson	4.00	1250	1341	408	11.5
9 mm	100	JHP	Speer	4.00	1315	1188	363	24.8
9 mm	115	FMJ	Browning	4.00	1140	1067	325	8.4
9 mm	115	FMJ	Smith+Wesson	4.00	1145	1192	363	11.8
9 mm	115	FMJ	Winchester	4.00	1140	1126	343	10.3
9 mm	115	JHP	Remington	4.00	1160	1192	363	28.2
9 mm	115	JHP	Smith+Wesson	4.00	1145	1193	363	20.4
9 mm	115	Power Point	Western Sup-X	4.00	1160	1272	387	9.4
9 mm	115	JHP(Silvertip)	Winchester	4.00	1225	1163	354	27.5[a]
9 mm	124	FMJ	Remington	4.00	1120	1084	330	11.3
9 mm	125	JSP	Speer	4.00	1120	1058	322	10.1
.357 Mag	110	JHP	Smith+Wesson	4.00	1800	1226	373	21.9
.357 Mag	110	JHP	Smith+Wesson	2.00	1800	1044	318	12.5
.357 Mag	110	JHP	Speer	4.00	1700	1246	379	28.7
.357 Mag	110	JHP	Speer	2.00	1700	1178	359	24.6
.357 Mag	110	JHP	Western Sup-X	4.00	1500	1309	398	29.9
.357 Mag	110	JHP	Western Sup-X	2.75	1500	1258	383	26.4
.357 Mag	125	JHP	Smith+Wesson	4.00	1775	1227	373	22.9
.357 Mag	125	JHP	Smith+Wesson	2.00	1775	1188	362	20.3
.357 Mag	125	JHP	Speer	4.00	1900	1301	396	39.7
.357 Mag	125	JHP	Speer	2.00	1900	1161	353	30.3
.357 Mag	125	JHP	Remington	4.00	1675	1366	416	40.8
.357 Mag	125	JHP	Remington	2.00	1675	1173	357	27.0
.357 Mag	140	JHP	Speer	4.00	1780	1221	372	41.8
.357 Mag	140	JHP	Speer	2.00	1780	1125	342	34.5
.357 Mag	158	JHP	Smith+Wesson	4.00	1050	1116	340	22.3
.357 Mag	158	JHP	Smith+Wesson	2.00	1050	982	299	14.6
.357 Mag	158	JSP	Federal	4.00	1550	1255	382	25.6
.357 Mag	158	JSP	Federal	2.00	1550	1195	364	21.5
.357 Mag	158	JSP	Smith+Wesson	4.00	1500	1168	356	19.2
.357 Mag	158	JSP	Smith+Wesson	2.00	1500	1091	332	15.1
.357 Mag	158	JSP	Speer	4.00	1625	1156	352	22.9
.357 Mag	158	JSP	Speer	2.00	1625	1030	313	16.6
.357 Mag	158	LRN	Western Sup-X	4.00	1410	1230	374	21.0
.357 Mag	158	LRN	Western Sup-X	2.00	1410	1169	356	16.7
.357 Mag	158	SWC	Remington	4.00	1410	1088	331	17.3
.357 Mag	158	SWC	Remington	2.00	1410	958	291	9.3
.38 Spec	90	JSP(Hemi)	Smith+Wesson	4.00	1350	1158	352	11.2
.38 Spec	90	JSP(Hemi)	Smith+Wesson	2.00	1350	1053	320	7.7
.38 Spec	90	JSP	Smith+Wesson	4.00	1350	1118	340	9.6
.38 Spec	90	JSP	Smith+Wesson	2.00	1350	975	297	6.1
.38 Spec	95	JHP(+P)	Remington	4.00	985	1187	361	28.9
.38 Spec	95	JHP(+P)	Remington	2.00	985	1019	310	16.4
.38 Spec	95	JHP(Silvertip +P)	Winchester	4.00	1100	1067	325	18.0[a]
.38 Spec	110	JHP	Smith+Wesson	4.00	1380	1014	309	11.3
.38 Spec	110	JHP	Smith+Wesson	2.00	1380	888	270	6.8
.38 Spec	110	JHP	Speer	4.00	1245	857	261	11.4
.38 Spec	110	JHP	Speer	2.00	1245	789	240	9.6

[a] RII calculated directly from Maximum Temporary Cavity Measurements.
[b] Advertised velocity.
[c] Velocity not available.

Abbreviations:
FMJ – Full Metal Jacket
JHP – Jacketed Hollow Point
JSP – Jacketed Soft Point
LHP – Lead Hollow Point
LRN – Lead Round Nose
SWC – Semi-Wadcutter
WC – Wadcutter

TABLE 1. *Predicted performance of commercially available handgun ammunition (continued).*

Cartridge	Bullet weight (grains)	Bullet type	Manufacturer	Barrel length (in)	Velocity Nominal[b] (fps)	Velocity Measured (fps)	Velocity Measured (mps)	Relative incapacitation index (RII)
.38 Spec	110	JHP	Super Vel	4.00	1370	1159	353	25.3
.38 Spec	110	JHP	Super Vel	2.00	1370	1148	349	24.8
.38 Spec	110	JHP(Lot-Q4070)	Winch-Western	4.00	[c]	1106	337	17.9
.38 Spec	110	JHP(Lot-Q4070)	Winch-Western	2.00	[c]	956	291	11.6
.38 Spec	110	JSP	Super Vel	4.00	1370	1202	366	19.2
.38 Spec	110	JSP	Super Vel	2.00	1370	1076	327	13.2
.38 Spec	125	JHP	Smith+Wesson	4.00	1350	900	274	5.9
.38 Spec	125	JHP	Smith+Wesson	2.00	1350	716	218	3.1
.38 Spec	125	JHP	Smith+Wesson	4.00	1350	1002	305	10.2
.38 Spec	125	JHP	Smith+Wesson	2.00	1350	899	274	5.8
.38 Spec	125	JHP(+P)	Speer	4.00	1425	1006	306	21.9
.38 Spec	125	JHP(+P)	Speer	2.00	1425	931	283	18.7
.38 Spec	125	JSP(+P)	Speer	4.00	1425	1047	319	19.4
.38 Spec	125	JSP(+P)	Speer	2.00	1425	983	299	16.7
.38 Spec	125	JSP	Smith+Wesson	4.00	1350	1064	324	15.4
.38 Spec	125	JSP	Smith+Wesson	2.00	1350	896	273	8.7
.38 Spec	125	JSP	3-D	4.00	1085	1091	332	16.7
.38 Spec	125	JSP	3-D	2.00	1085	957	291	10.8
.38 Spec	125	JHP	Remington	4.00	1160	1108	337	23.2
.38 Spec	125	JHP	Remington	2.00	1160	911	277	13.9
.38 Spec	140	JHP(+P)	Speer	4.00	1200	978	298	23.0
.38 Spec	140	JHP(+P)	Speer	2.00	1200	897	273	17.0
.38 Spec	148	WC	Browning	4.00	770	731	222	13.9
.38 Spec	148	WC	Browning	2.00	770	618	188	12.2
.38 Spec	148	WC	Remington	4.00	770	741	225	15.9
.38 Spec	148	WC	Remington	2.00	770	700	213	15.3
.38 Spec	148	WC	Federal	4.00	770	737	224	14.0
.38 Spec	148	WC	Federal	2.00	674	770	205	13.0
.38 Spec	148	WC	Smith+Wesson	4.00	726	800	221	9.0
.38 Spec	148	WC	Smith+Wesson	2.00	662	800	201	8.0
.38 Spec	148	WC	Speer	4.00	679	825	206	13.1
.38 Spec	148	WC	Speer	2.00	652	825	198	12.7
.38 Spec	148	WC	Western	4.00	696	770	212	13.7
.38 Spec	148	WC	Western	2.00	618	770	188	12.6
.38 Spec	158	JHP	Smith+Wesson	4.00	1047	1050	319	18.2
.38 Spec	158	JHP	Smith+Wesson	2.00	950	1050	289	12.9
.38 Spec	158	JSP	Smith+Wesson	4.00	828	1050	252	5.5
.38 Spec	158	JSP	Smith+Wesson	2.00	730	1050	222	3.3
.38 Spec	158	LRN	Winchester	4.00	919	855	280	7.5
.38 Spec	158	LRN	Winchester	2.00	780	855	237	5.5
.38 Spec	158	LRN(+P)	Federal	4.00	999	1090	304	8.6
.38 Spec	158	LRN(+P)	Federal	2.00	947	1090	288	7.2
.38 Spec	158	LRN	Federal	4.00	795	855	242	4.8
.38 Spec	158	LRN	Federal	2.00	632	855	192	3.8
.38 Spec	158	LRN	Remington	4.00	749	855	228	6.1
.38 Spec	158	LRN	Remington	2.00	694	855	211	5.7
.38 Spec	158	LRN	Speer	4.00	749	975	228	4.4
.38 Spec	158	LRN	Speer	2.00	635	975	193	3.8
.38 Spec	158	LRN	Smith+Wesson	4.00	708	910	215	1.5

[a] RII calculated directly from Maximum Temporary Cavity Measurements.
[b] Advertised velocity.
[c] Velocity not available.

Abbreviations:
FMJ – Full Metal Jacket
JHP – Jacketed Hollow Point
JSP – Jacketed Soft Point
LHP – Lead Hollow Point
LRN – Lead Round Nose
SWC – Semi-Wadcutter
WC – Wadcutter

TABLE 1. *Predicted performance of commercially available handgun ammunition (continued).*

Cartridge	Bullet weight (grains)	Bullet type	Manufacturer	Barrel length (in)	Velocity Nominal[b] (fps)	Velocity Measured (fps)	Velocity Measured (mps)	Relative incapacitation index (RII)
.38 Spec	158	LRN	Smith+Wesson	2.00	910	626	190	1.2
.38 Spec	158	LHP	Winch-Western	4.00	855	915	278	17.2
.38 Spec	158	LHP	Winch-Western	2.00	855	805	245	11.5
.38 Spec	158	SWC	Federal	4.00	855	823	250	6.7
.38 Spec	158	SWC	Federal	2.00	855	796	242	5.7
.38 Spec	158	SWC	Smith+Wesson	4.00	1060	875	266	3.9
.38 Spec	158	SWC	Smith+Wesson	4.00	850	1006	306	10.8
.38 Spec	158	SWC	Smith+Wesson	2.00	850	870	265	3.7
.38 Spec	158	SWC	Speer	4.00	975	803	244	10.0
.38 Spec	158	SWC	Speer	2.00	975	640	195	5.7
.38 Spec	158	SWC	Winchester	4.00	855	924	281	14.2
.38 Spec	158	SWC	Winchester	2.00	855	799	237	8.8
.38 Spec	200	LRN	Remington	4.00	730	647	197	2.9
.38 Spec	200	LRN	Remington	2.00	730	593	180	2.3
.38 Spec	200	LRN	Speer	4.00	850	710	216	3.8
.38 Spec	200	LRN	Speer	2.00	850	598	182	2.4
.38 Spec	200	LRN	Western Sup-X	4.00	730	626	190	2.7
.38 Spec	200	LRN	Western Sup-X	2.00	730	592	180	2.4
.41 Mag	210	JSP	Remington	4.00	1500	1260	384	51.6
.41 Mag	210	SWC	Remington	4.00	1050	944	287	6.2
.44 Mag	180	JSP	Super Vel	4.00	1995	1495	455	33.5
.44 Mag	200	JHP	Speer	4.00	1675	1277	389	67.3
.44 Mag	240	JHP	Browning	4.00	1330	1257	383	50.1
.44 Mag	240	JHP	Remington	4.00	1470	1229	374	47.3
.44 Mag	240	JSP	Speer	4.00	1650	1203	366	49.0
.44 Mag	240	SWC	Browning	4.00	1470	1311	399	32.9
.44 Mag	240	SWC	Remington	4.00	1470	1286	391	32.2
.44 Mag	240	SWC	Winch-Western	4.00	1470	1330	405	33.4
.45 Auto	185	JHP	Remington	5.00	950	895	272	18.0
.45 Auto	185	JHP(Silvertip)	Winchester	5.00	1000	989	301	25.5[a]
.45 Auto	185	WC	Remington	5.00	775	821	250	3.5
.45 Auto	185	WC	Federal	5.00	775	751	228	6.3
.45 Auto	230	FMJ	Remington	5.00	810	864	263	4.3
.45 Auto	230	FMJ	Winch-Western	5.00	810	800	244	3.6
.45 LC	255	LRN	Winch-Western	7.50	860	821	250	3.7

[a] RII calculated directly from Maximum Temporary Cavity Measurements.
[b] Advertised velocity.
[c] Velocity not available.

Abbreviations:
FMJ – Full Metal Jacket
JHP – Jacketed Hollow Point
JSP – Jacketed Soft Point
LHP – Lead Hollow Point
LRN – Lead Round Nose
SWC – Semi-Wadcutter
WC – Wadcutter

TABLE 2. *Predicted performance of commercially available handgun ammunition. RII arranged in descending order within bullet caliber.*

Cartridge	Bullet weight (grains)	Bullet type	Manufacturer	Barrel length (in)	Velocity			Relative incapacitation index (RII)
					Nominal[b] (fps)	Measured (fps)	(mps)	
380 Auto	85	JHP(Silvertip)	Winchester	3.88	1000	986	300	13.4[a]
9 mm	115	JHP	Remington	4.00	1160	1192	363	28.2
9 mm	115	JHP(Silvertip)	Winchester	4.00	1225	1163	354	27.5[a]
9 mm	100	JHP	Speer	4.00	1315	1188	363	24.8
9 mm	115	JHP	Smith+Wesson	4.00	1145	1193	363	20.4
9 mm	115	FMJ	Smith+Wesson	4.00	1145	1192	363	11.8
9 mm	100	FMJ	Smith+Wesson	4.00	1250	1341	408	11.5
9 mm	124	FMJ	Remington	4.00	1120	1084	330	11.3
9 mm	115	FMJ	Winchester	4.00	1140	1126	343	10.3
9 mm	125	JSP	Speer	4.00	1120	1058	322	10.1
9 mm	115	Power Point	Western Sup-X	4.00	1160	1272	387	9.4
9 mm	115	FMJ	Browning	4.00	1140	1067	325	8.4
.357 Mag	140	JHP	Speer	4.00	1780	1221	372	41.8
.357 Mag	125	JHP	Remington	4.00	1675	1366	416	40.8
.357 Mag	125	JHP	Speer	4.00	1900	1301	396	39.7
.357 Mag	140	JHP	Speer	2.00	1780	1125	342	34.5
.357 Mag	125	JHP	Speer	2.00	1900	1161	353	30.3
.357 Mag	110	JHP	Western Sup-X	4.00	1500	1309	398	29.9
.357 Mag	110	JHP	Speer	4.00	1700	1246	379	28.7
.357 Mag	125	JHP	Remington	2.00	1675	1173	357	27.0
.357 Mag	110	JHP	Western Sup-X	2.75	1500	1258	383	26.4
.357 Mag	158	JSP	Federal	4.00	1550	1255	382	25.6
.357 Mag	110	JHP	Speer	2.00	1700	1178	359	24.6
.357 Mag	125	JHP	Smith+Wesson	4.00	1775	1227	373	22.9
.357 Mag	158	JSP	Speer	4.00	1625	1156	352	22.9
.357 Mag	158	JHP	Smith+Wesson	4.00	1050	1116	340	22.3
.357 Mag	110	JHP	Smith+Wesson	4.00	1800	1226	373	21.9
.357 Mag	158	JSP	Federal	2.00	1550	1195	364	21.5
.357 Mag	158	LRN	Western Sup-X	4.00	1410	1230	374	21.0
.357 Mag	125	JHP	Smith+Wesson	2.00	1775	1188	362	20.3
.357 Mag	158	JSP	Smith+Wesson	4.00	1500	1168	356	19.2
.357 Mag	158	SWC	Remington	4.00	1410	1088	331	17.3
.357 Mag	158	LRN	Western Sup-X	2.00	1410	1169	356	16.7
.357 Mag	158	JSP	Speer	2.00	1625	1030	313	16.6
.357 Mag	158	JSP	Smith+Wesson	2.00	1500	1091	332	15.1
.357 Mag	158	JHP	Smith+Wesson	2.00	1050	982	299	14.6
.357 Mag	110	JHP	Smith+Wesson	2.00	1800	1044	318	12.5
.357 Mag	158	SWC	Remington	2.00	1410	958	291	9.3
.38 Spec	95	JHP(+P)	Remington	4.00	985	1187	361	28.9
.38 Spec	110	JHP	Super Vel	4.00	1370	1159	353	25.3
.38 Spec	110	JHP	Super Vel	2.00	1370	1148	349	24.8
.38 Spec	125	JHP	Remington	4.00	1160	1108	337	23.2
.38 Spec	140	JHP(+P)	Speer	4.00	1200	978	298	23.0
.38 Spec	125	JHP(+P)	Speer	4.00	1425	1006	306	21.9
.38 Spec	125	JSP(+P)	Speer	4.00	1425	1047	319	19.4
.38 Spec	110	JSP	Super Vel	4.00	1370	1202	366	19.2
.38 Spec	125	JHP(+P)	Speer	2.00	1425	921	283	18.7
.38 Spec	158	JHP	Smith+Wesson	4.00	1050	1047	319	18.2
.38 Spec	95	JHP(Silvertip +P)	Winchester	4.00	1100	1067	325	18.0[a]

[a] RII calculated directly from Maximum Temporary Cavity Measurements.
[b] Advertised velocity.
[c] Velocity not available.

Abbreviations:

FMJ – Full Metal Jacket
JHP – Jacketed Hollow Point
JSP – Jacketed Soft Point
LC – Long Colt
LHP – Lead Hollow Point
LRN – Lead Round Nose
SWC – Semi-Wadcutter
WC – Wadcutter

TABLE 2. *Predicted performance of commercially available handgun ammunition. RII arranged in descending order within bullet caliber (continued).*

Cartridge	Bullet weight (grains)	Bullet type	Manufacturer	Barrel length (in)	Velocity			Relative incapacitation index (RII)
					Nominal[b] (fps)	Measured (fps)	(mps)	
.38 Spec	110	JHP(Lot-Q4070)	Winch-Western	4.00	c	1106	337	17.9
.38 Spec	158	LHP	Winch-Western	4.00	855	915	278	17.2
.38 Spec	140	JHP(+P)	Speer	2.00	1200	897	273	17.0
.38 Spec	125	JSP	3-D	4.00	1085	1091	332	16.7
.38 Spec	125	JSP(+P)	Speer	2.00	1425	983	299	16.7
.38 Spec	95	JHP(+P)	Remington	2.00	985	1019	310	16.4
.38 Spec	148	WC	Remington	4.00	770	741	225	15.9
.38 Spec	125	JSP	Smith+Wesson	4.00	1350	1064	324	15.4
.38 Spec	148	WC	Remington	2.00	770	700	213	15.3
.38 Spec	158	SWC	Winchester	4.00	855	924	281	14.2
.38 Spec	148	WC	Federal	4.00	770	737	224	14.0
.38 Spec	125	JHP	Remington	2.00	1160	911	277	13.9
.38 Spec	148	WC	Browning	4.00	770	731	222	13.9
.38 Spec	148	WC	Western	4.00	770	696	212	13.7
.38 Spec	110	JSP	Super Vel	2.00	1370	1076	327	13.2
.38 Spec	148	WC	Speer	4.00	825	679	206	13.1
.38 Spec	148	WC	Federal	2.00	770	674	205	13.0
.38 Spec	158	JHP	Smith+Wesson	2.00	1050	950	289	12.9
.38 Spec	148	WC	Speer	2.00	825	652	198	12.7
.38 Spec	148	WC	Western	2.00	770	618	188	12.6
.38 Spec	148	WC	Browning	2.00	770	618	188	12.2
.38 Spec	110	JHP(Lot-Q4070)	Winch-Western	2.00	c	956	291	11.6
.38 Spec	158	LHP	Winch-Western	2.00	855	805	245	11.5
.38 Spec	110	JHP	Speer	4.00	1245	857	261	11.4
.38 Spec	110	JHP	Smith+Wesson	4.00	1380	1014	309	11.3
.38 Spec	90	JSP(Hemi)	Smith+Wesson	4.00	1350	1158	352	11.2
.38 Spec	158	SWC	Smith+Wesson	4.00	850	1006	306	10.8
.38 Spec	125	JSP	3-D	2.00	1085	957	291	10.8
.38 Spec	125	JHP	Smith+Wesson	4.00	1350	1002	305	10.2
.38 Spec	158	SWC	Speer	4.00	975	803	244	10.0
.38 Spec	90	JSP	Smith+Wesson	4.00	1350	1118	340	9.6
.38 Spec	110	JHP	Speer	2.00	1245	789	240	9.6
.38 Spec	148	WC	Smith+Wesson	4.00	800	726	221	9.0
.38 Spec	158	SWC	Winchester	2.00	855	799	237	8.8
.38 Spec	125	JSP	Smith+Wesson	2.00	1350	896	273	8.7
.38 Spec	158	LRN(+P)	Federal	4.00	1090	999	304	8.6
.38 Spec	148	WC	Smith+Wesson	2.00	800	662	201	8.0
.38 Spec	90	JSP(Hemi)	Smith+Wesson	2.00	1350	1053	320	7.7
.38 Spec	158	LRN	Winchester	4.00	855	919	280	7.5
.38 Spec	158	LRN(+P)	Federal	2.00	1090	947	288	7.2
.38 Spec	110	JHP	Smith+Wesson	2.00	1380	888	270	6.8
.38 Spec	158	SWC	Federal	4.00	855	823	250	6.7
.38 Spec	90	JSP	Smith+Wesson	2.00	1350	975	297	6.1
.38 Spec	158	LRN	Remington	4.00	855	749	228	6.1
.38 Spec	125	JHP	Smith+Wesson	4.00	1350	900	274	5.9
.38 Spec	125	JHP	Smith+Wesson	2.00	1350	899	274	5.8
.38 Spec	158	SWC	Federal	2.00	855	796	242	5.7
.38 Spec	158	LRN	Remington	2.00	855	694	211	5.7
.38 Spec	158	SWC	Speer	2.00	975	640	195	5.7

[a] RII calculated directly from Maximum Temporary Cavity Measurements.
[b] Advertised velocity.
[c] Velocity not available.

Abbreviations:

FMJ – Full Metal Jacket
JHP – Jacketed Hollow Point
JSP – Jacketed Soft Point
LC – Long Colt
LHP – Lead Hollow Point
LRN – Lead Round Nose
SWC – Semi-Wadcutter
WC – Wadcutter

TABLE 2. *Predicted performance of commercially available handgun ammunition. RII arranged in descending order within bullet caliber (continued).*

Cartridge	Bullet weight (grains)	Bullet type	Manufacturer	Barrel length (in)	Velocity			Relative incapacitation index (RII)
					Nominal[b] (fps)	Measured (fps)	(mps)	
.38 Spec	158	JSP	Smith+Wesson	4.00	1050	828	252	5.5
.38 Spec	158	LRN	Winchester	2.00	855	780	237	5.5
.38 Spec	158	LRN	Federal	4.00	855	795	242	4.8
.38 Spec	158	LRN	Speer	4.00	975	749	228	4.4
.38 Spec	158	SWC	Smith+Wesson	4.00	1060	875	266	3.9
.38 Spec	200	LRN	Speer	4.00	850	710	216	3.8
.38 Spec	158	LRN	Speer	2.00	975	635	193	3.8
.38 Spec	158	LRN	Federal	2.00	855	632	192	3.8
.38 Spec	158	SWC	Smith+Wesson	2.00	850	870	265	3.7
.38 Spec	158	JSP	Smith+Wesson	2.00	1050	730	222	3.3
.38 Spec	125	JHP	Smith+Wesson	2.00	1350	716	218	3.1
.38 Spec	200	LRN	Remington	4.00	730	647	197	2.9
.38 Spec	200	LRN	Western Sup-X	4.00	730	626	190	2.7
.38 Spec	200	LRN	Speer	2.00	850	598	182	2.4
.38 Spec	200	LRN	Western Sup-X	2.00	730	592	180	2.4
.38 Spec	200	LRN	Remington	2.00	730	593	180	2.3
.38 Spec	158	LRN	Smith+Wesson	4.00	910	708	215	1.5
.38 Spec	158	LRN	Smith+Wesson	2.00	910	626	190	1.2
.41 Mag	210	JSP	Remington	4.00	1500	1260	384	51.6
.41 Mag	210	SWC	Remington	4.00	1050	944	287	6.2
.44 Mag	200	JHP	Speer	4.00	1675	1277	389	67.3
.44 Mag	240	JHP	Browning	4.00	1330	1257	383	50.1
.44 Mag	240	JSP	Speer	4.00	1650	1203	366	49.0
.44 Mag	240	JHP	Remington	4.00	1470	1229	374	47.3
.44 Mag	180	JSP	Super Vel	4.00	1995	1495	455	33.5
.44 Mag	240	SWC	Winch-Western	4.00	1470	1330	405	33.4
.44 Mag	240	SWC	Browning	4.00	1470	1311	399	32.9
.44 Mag	240	SWC	Remington	4.00	1470	1286	391	32.2
.45 Auto	185	JHP(Silvertip)	Winchester	5.00	1000	989	301	25.5[a]
.45 Auto	185	JHP	Remington	5.00	950	895	272	18.0
.45 Auto	185	WC	Federal	5.00	775	751	228	6.3
.45 Auto	230	FMJ	Remington	5.00	810	864	263	4.3
.45 Auto	230	FMJ	Winch-Western	5.00	810	800	244	3.6
.45 Auto	185	WC	Remington	5.00	775	821	250	3.5
.45 LC	255	LRN	Winch-Western	7.50	860	821	250	3.7

[a] RII calculated directly from Maximum Temporary Cavity Measurements.
[b] Advertised velocity.
[c] Velocity not available.

Abbreviations:

FMJ – Full Metal Jacket
JHP – Jacketed Hollow Point
JSP – Jacketed Soft Point
LC – Long Colt
LHP – Lead Hollow Point
LRN – Lead Round Nose
SWC – Semi-Wadcutter
WC – Wadcutter

POLICE HANDGUN AMMUNITION: INCAPACITATION EFFECTS VOLUME I: EVALUATION

William J. Bruchey, Jr.*

U.S. Army Armament Research and Development Command, Aberdeen Proving Ground, MD 21005

and

Daniel E. Frank**

National Bureau of Standards, Washington, DC 20234

This report presents the results of an experimental evaluation of handgun ammunition in calibers from 9 mm to 45 for use by law enforcement personnel. An evaluation criterion called the Relative Incapacitation Index (RII) is defined. Commercially loaded cartridges are ranked in effectiveness according to the RII. Computer simulation is used to evaluate two different aim points, the effects of shooter accuracy, and the efficiency of nondeforming projectiles.

Key words: ammunition; bullets; cavity formation; handgun ammunition; incapacitation; penetration; relative incapacitation index; small arms; tissue simulant.

INTRODUCTION

In December 1972, the National Institute of Justice (NIJ) of the U.S. Department of Justice (then known as the National Institute of Law Enforcement and Criminal Justice) approved and funded a project, submitted by the Law Enforcement Standards Laboratory (LESL) of the National Bureau of Standards, to conduct a study of the terminal effects of police handgun ammunition. LESL, in 1973, contracted with the U.S. Army Ballistic Research Laboratory (BRL) to conduct the study and prepare a report of its findings. The purpose of the study was to provide Federal, State, and local law enforcement agencies with criteria for use in selection of handgun ammunition. The study attempted to bring the salient features of previous studies together with a more detailed and updated description of the entire scenario to produce a unified approach to the evaluation of handgun ammunition effectiveness. This work was first documented in a summary report in 1975 [1].† Additional tests were conducted in the summer and fall of 1981 to examine the performance of selected ammunition introduced since 1975 and to verify certain of the test results.

This report describes the study work that has led to a new criterion for evaluating and estimating the expected performance of handgun cartridges used for law enforcement purposes. It postulates that a law enforcement officer requires a defensive system that produces immediate incapacitation of an assailant rather than eventual death. The report describes the terminal characteristics of police handgun bullets and their relationship to incapacitation.

The original project plan for this study included provisions to determine the ricochet potential of the various bullet constructions and a measure of the hazard to bystanders of ricocheting projectiles. While the data collected for these purposes were interesting, they did not provide conclusive evidence on which to base any predictions. It was therefore decided not to report the data at this time and to save the entire question of ricochet and ricochet hazard potential for future studies.

*Ballistic Research Laboratory.

**Law Enforcement Standards Laboratory, National Engineering Laboratory.

† Numbers in brackets refer to the references in appendix A.

BACKGROUND

A number of theories on the subject of stopping power or incapacitation performance have been proposed over the years. Perhaps the best known is the Hatcher theory. General Hatcher [2], in 1935 proposed that an indication of the incapacitation potential of a kinetic energy projectile was proportional to impact momentum times the bullet's cross-sectional area. He called this incapacitation potential, or stopping power. In 1960, and again in 1969, the U.S. Army advanced the theory that incapacitation was a function of the kinetic energy deposited in 15 cm of gelatin tissue simulant [3]. More recently, DeMaio [4] has applied this kinetic energy theory to handgun effectiveness.

Each of these theories on incapacitation has certain shortcomings. Hatcher's theory is based only on the striking conditions of the bullet, i.e., its mass, velocity, and caliber. It considers that a bullet striking anywhere on the body with a fixed set of parameters will produce the same effect. The kinetic energy deposit theory is an advancement over the Hatcher theory. It considers that only the portion of the bullet's energy deposited in the assailant is capable of effecting incapacitation. Its primary drawback is that energy deposited anywhere in the body is considered to be equally effective. The intent of the present effort is to draw together the two theories, eliminate the weaknesses of each, and propose a more comprehensive model in the light of current knowledge.

The measure of potential incapacitation capability, called the Relative Incapacitation Index (RII), developed during this study considers:

1. The ability of the average police officer to deliver effective fire.
2. The relative effectiveness of hits at different locations on a human target.
3. "Rapid incapacitation" (since all the results in this study are based on average performance "one shot incapacitation" cannot be guaranteed).
4. The performance of bullets (Terminal Ballistics) in a reproducible target medium.
5. A requirement to be able to extend the RII to variations in cartridge loadings without an extensive new test program.

MARKSMANSHIP

It is axiomatic that a bullet that does not hit the target is worthless. Further, all real shooters, unlike their television counterparts, recognize that even if one "hits the target," not all of the shots will hit exactly the same spot on the target or even the desired area of the target. There are several types of errors that contribute to this condition. The two types of errors examined in this report are shooter error and ammunition error. For the purposes of this report the difference between the actual impact point of a bullet on a target and the desired impact point is called the firing error and includes both the shooter and ammunition errors.

The Ballistic Research Laboratory was not expected to generate experimental data on firing errors. However, two sets of data were available from other sources that cover firing errors. The first set of data was made available by the Human Engineering Laboratories (HEL) at Aberdeen Proving Grounds (APG) [5]. It consists of the impact error as a function of range for soldiers firing the M1911A1 pistol under "stress" conditions; i.e., the soldiers, identified as Group A, were instructed that their prime purpose was to hit a pop-up silhouette target as quickly as possible after exposure. These targets appeared in random sequences out to a range of 30 m.

The second set of data was taken from a report prepared by the H. P. White Laboratories for the U.S. Army Land Warfare Laboratory (LWL) at APG [6]. These tests consisted of timed fire by highly trained police officers, identified as Group B, using 38 Special revolvers. B-21 silhouette targets were used.

The composite curves of firing error versus range for both sets of data are shown in figure 1. As can be seen, the Group A curve lies considerably higher than the Group B curves. The difference in level between the two curves is due primarily to the test conditions since both groups were familiar with their weapons. Timed fire at an exposed silhouette target is less difficult than firing at randomly exposed targets. It is felt that the conditions experienced by Group A more closely approximate those encountered in law enforcement situations; consequently, Group A data were used as the basic hit distribution for this study.

DATA BASE	σ_0		b	
	Hor.	Vert.	Hor.	Vert.
Group A	38.4	38.4	0.02325	0.02325
Group B	27.6	18.0	0.04627	0.03770

$\sigma = \sigma_0 \text{ EXP } (-b \cdot \text{RANGE})$

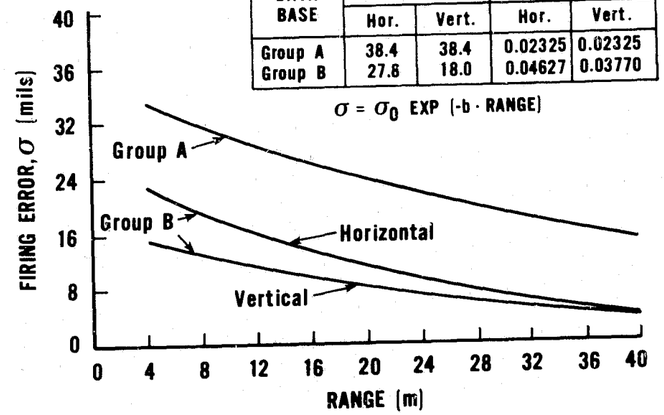

FIGURE 1. *Firing error as a function of engagement range.*

The second factor to be observed from these two curves is that firing error decreases as range increases. This observation is consistent with independent tests conducted in other small arms studies. Conjecture is that this phenomenon is due to the shooter taking more deliberate aim and making better use of the gun sights, especially at longer ranges; thus, as the range increases, the "point and fire" tendency of the shooter is replaced by "aim and fire."

Figures 2 through 4 show the Group A hit distribution on a silhouette of a human torso for a random sample of 240 shots. The ranges correspond to the average engagement range, 6 m (approximately 20 ft), and one-half and double this value. The circles show separate regions of miss distance about the aim point, denoted by the "X" in the figure. The zones correspond to:

Zone 1—The innermost circle, with a radius of one standard deviation. Shots impacting in this zone have a miss distance of less than one standard deviation.

Zone 2—The area outside Zone 1 but within the outermost circle, with a radius of two standard deviations. Shots impacting in this zone have a miss distance of more than one but less than two standard deviations.

Zone 3—The area outside of Zone 2. Shots impacting in this zone have a miss distance greater than two standard deviations.

These figures are illustrative only, and are presented to give the reader an appreciation for the locations of impact points on a human torso and a visual picture of the magnitude of the possible firing errors involved.

As stated previously, the firing error, as depicted in figure 1 contains contributions due to the shooter and the ammunition/weapon used. Data gathered in previous studies show that shooter error and ammunition error can be treated as statistically independent; that is, the square of the standard deviation of the firing error, σ_f, is the sum of the squares of the standard deviation of the shooter error, σ_s, and the standard deviation of the ammunition error, σ_a, i.e.,

$$\sigma_f^2 = \sigma_s^2 + \sigma_a^2$$

The Group A and Group B data do not indicate what part of σ_f is due to the shooter and what part is due to ammunition. To determine the importance of σ_a as it affects stopping power and how it varies with weapon, choice of ammunition, bullet velocity, etc., a series of tests was conducted to measure σ_a.

The ammunition used consisted of more than 100 different types (i.e., bullet construction, manufacturer, and mass). The weapons were fired from a machine rest at paper targets (28×36

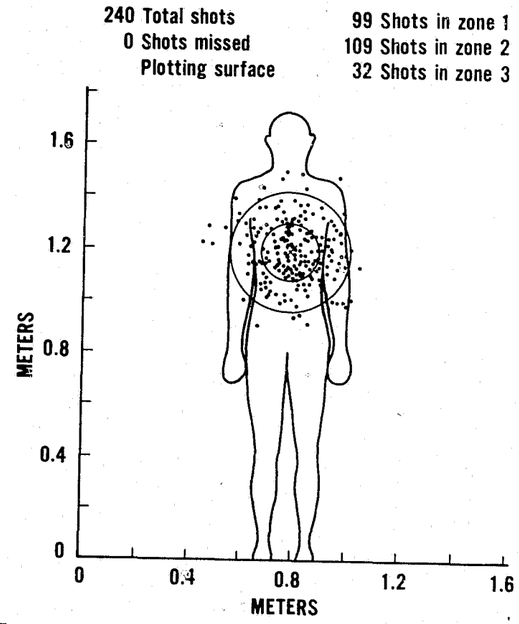

FIGURE 2. *Group A hit distribution superimposed on a computer man silhouette at 3-m range.*

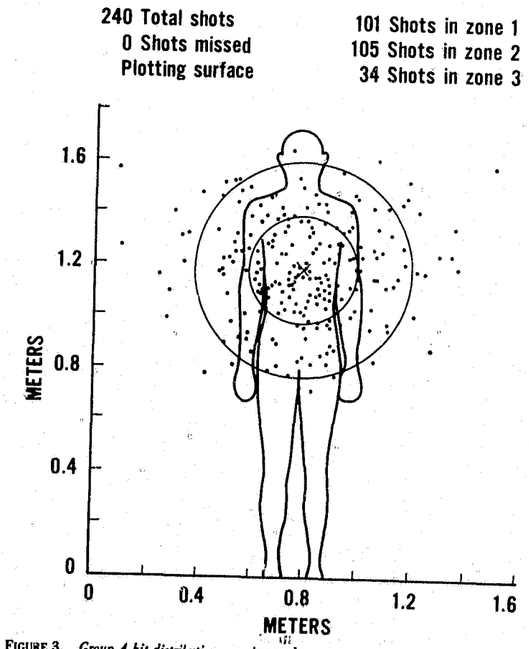

FIGURE 3. *Group A hit distribution superimposed on a computer man silhouette at 6-m range.*

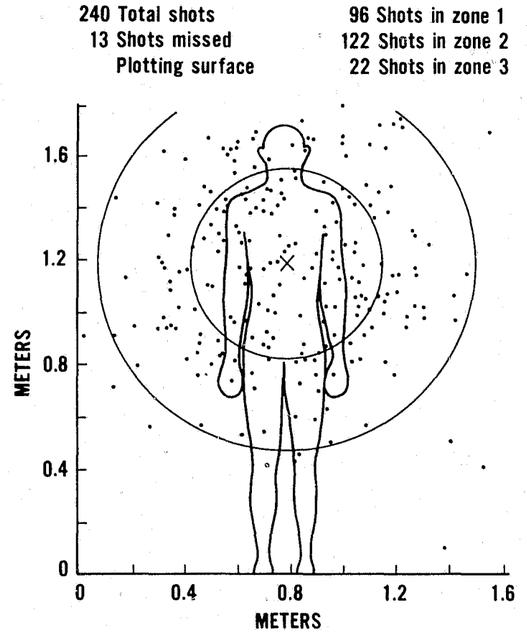

FIGURE 4. *Group A hit distribution superimposed on a computer man silhouette at 12-m range.*

cm) 15 m away. The vertical and horizontal impact points on the target were measured from an arbitrary reference point. The standard deviation, S.D., of the shots about the center of the shot pattern was then computed. This was then converted to mils, denoted σ_s, by the formula:

$$\sigma_s = \frac{\text{S.D.(cm)}}{\text{Range(cm)}} \times 1000$$

For the over 100 different tests run, with one exception, the average ammunition error was 0.98 mils with a standard deviation of 0.8 mils. The total firing error, σ_f, for ranges from 3 to 12 m, varies from 35 to 30 mils for Group A and 23 to 16 mils for the Group B data. Using the average σ_f value, the percent of the total firing error, σ_f, attributable to the ammunition was less than 1 percent.

The conclusion based on these data is that for the weapons used (ones in good condition and various calibers) the inherent inaccuracy of ammunition among manufacturers, bullet types, and bullet velocity levels is not significant when compared to the shooter error. In other words, ammunition accuracy far exceeds shooter accuracy. This conclusion should not be interpreted as saying that total firing error, σ_f, is independent of recoil level associated with a given weapon/ammunition combination. In fact, we would expect that there could be a strong correlation. For example, with respect to the average police officer, it would be expected that shooter errors are greater when firing the 44 Magnum cartridge particularly for a rapid second shot as compared to the 38 Special cartridge even though the inherent accuracy of the ammunition was approximately the same in both cases. Recoil effects on shooter accuracy were not addressed in this study but its effects could be investigated in a subsequent effort.

The one exception to the above discussion concerning the importance of ammunition error was the data obtained during the tests conducted using the MB Associates' Short Stop Cartridge. Only a limited number of cartridges were available at the time of testing. When fired from a machine rested revolver at a distance of 15 m at a target, 28 × 36 cm, insufficient hits on the

target were obtained to permit computations of ammunition errors. Consequently, as opposed to conventional ammunition, the accuracy of these rounds could adversely affect the performance of the weapon/shooter combination being considered. At this time, it is not known if this inaccuracy is inherent in this cartridge or if there was a quality control problem with the particular ammunition tested.

THE "COMPUTER MAN"

The second factor to be considered in the development of a Relative Incapacitation Index is the relative effectiveness of hits at different locations on a human target. This part of the study was accomplished through a combination of practical medical experience coupled with computer simulation of the interaction of shooter Group A firing data with a computerized representation of the human body, called the "Computer Man."

The computer man is an elaborate three-dimensional computer code of the human anatomy [7]. It consists of volume elements of the body of a person in the form of a rectangular parallelepiped approximately 5×5×25 mm high. A frontal view of the computer man, depicting the horizontal sectioning of the body, as he would "appear" in the computer is shown in figure 5. It should be noted that the figure is intended only as a concept of the torso sectioning and is not to scale. Within each of these volume elements, the predominant tissue type was identified and encoded. For the purpose of this study, each of these volume elements was assessed by a team of physicians from the University of Maryland Shock Trauma Unit as to its relative importance to incapacitation and as such were called Injury Criteria Component Vulnerability Numbers [8].

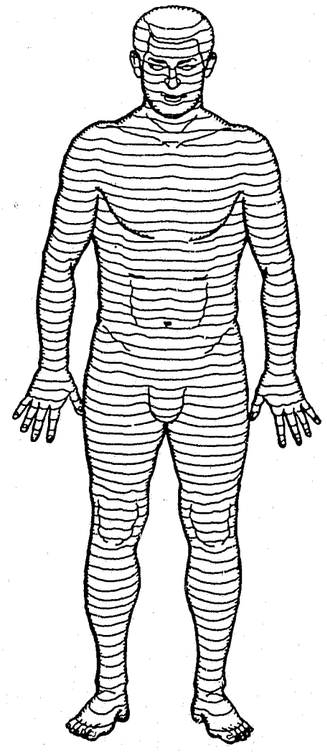

FIGURE 5. *Sketch of the Computer Man.*

The assessment by the physicians was based on a probable situation in which an officer would employ his handgun. The engagement range is short (7 m or less), and time is minimal. In this situation the officer cannot wait hours, minutes, or even 30 s for aggression to stop. What is desired is a weapon/cartridge combination that will, with a well placed shot, render the felon immediately noncombatant.

Within this framework, the doctors were presented with the following scenario:

> An armed felon has been placed in a situation where he feels that only an act of aggression on his part will prevent the loss of his life or that his freedom can be gained only through a violent action directed at the law enforcement officer. The felon is armed with some type of hand-held lethal weapon (pistol, knife, club, brick, etc.) and is being approached by the officer. In this situation the officer must administer an instantaneous incapacitating injury to the felon.

Each doctor was then asked to rank each volume element of the Computer Man as to its overall importance to instant incapacitation. A top view of a typical horizontal cross section showing the numerically ranked volume elements through a shoulder section of the Computer Man is depicted in figure 6. As in figure 5, figure 6 is intended only to convey the concept of the volume elements; it is not to scale. The computer man actually contains far more volume elements than shown here. The numerical scores range from 0–10; that is, they range from no importance to one of extreme importance relative to incapacitation. The complete set of these numbers, called Component Vulnerability Numbers, results in a three-dimensional mapping of the human body, with each element numerically coded in accordance with its relative importance to incapacitation.

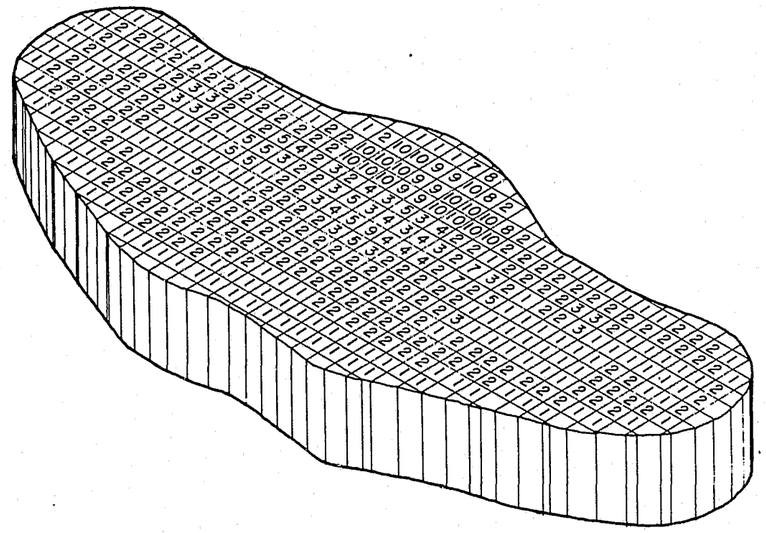

FIGURE 6. *Top view of typical cross section of the Computer Man (shoulder region).*

For a weapon, shooter, and ammunition combination, the different areas of the body do not have equal probabilities of impact. To account for this effect, a hit distribution characterizing the ability of a shooter/weapon/ammunition combination to place a well aimed shot (as discussed in the previous section on marksmanship) is used during simulated weapon fire against the Computer Man as the target.

The spatial distribution of possible trajectories for the bullets is characterized by the engagement range and standard deviation of shots about the aim point. Using the standard deviation of the shots and the assumption that shots are normally distributed about the aim point,

a statistical sampling technique, Monte Carlo Sampling, was used to generate a distribution of directions and impact points for a set of shots "fired" at the Computer Man. That is, the computer simulates the range of trajectories of individual shots fired by the shooter and traces each shot through the Computer Man. In all cases, the computer simulation assumes a forward torso entry point.

As each trajectory is being traced through the torso, the computer keeps track of the component vulnerability number assigned to each volume element along the trajectory at each increment of penetration. The component vulnerability numbers at each increment of penetration for all of the shots in the set are averaged to generate the average vulnerability called the V. Ind. function. It should be noted at this point that the model simulates the average environment of the bullet for the entire set of shots. The model does this by using zeros for the component vulnerability numbers along the whole trajectory whenever a "shot" misses the Computer Man.

If one were to keep track of the average value of the vulnerability component at any one particular depth of penetration after each shot fired, the average value would with each simulated "shot" increase or decrease. However, it was determined that after 10,000 "shots" the average vulnerability value at each depth stabilized (i.e., did not change appreciably with additional shots). Therefore, the average vulnerability vs. depth of penetration curves presented in this report are the result of 10,000 simulated shots. The V. Ind. function for Group A shooters at 6 m is shown graphically as figure 7 and is tabulated as part of the example in the sample calculation section of this report. The stabilized V. Ind. function, varies significantly, depending upon the statistical distribution of shot trajectories that result from different shooter's accuracy or engagement ranges. Appendix D presents the result of studies to determine the V. Ind. functions for varying marksmanship at various ranges and for different aim points.

The primary objective of this study, however, was to establish a criterion that would enable the comparison of police handgun ammunition in terms of the relative incapacitation performance of different cartridges. To do so requires that those variables that are independent of the bullet interaction with the target be fixed so that all bullets are then judged against a single measure of performance. With this in mind, the V. Ind. function shown in figure 7 was selected as representative of the average vulnerability of the human body combined with the average marksmanship potential for shots fired by law enforcement personnel in a typical engagement situation. Having selected a single V. Ind. function, it remains to combine the interaction of bullets with the target, in this study tissue simulant, to establish the relative performance of different types of police handgun ammunition.

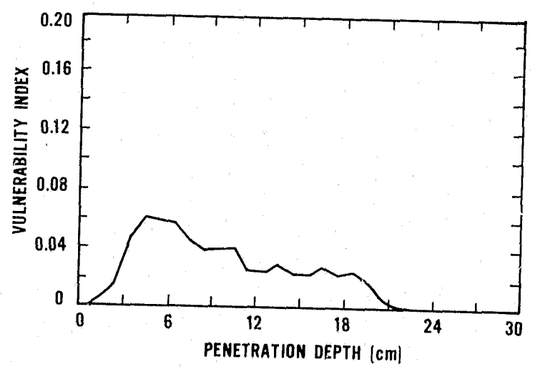

FIGURE 7. *Vulnerability index for handguns at a range of 6 m for the Group A hit distribution.*

TERMINAL BALLISTICS

Maximum Temporary Cavity

DeMaio in his article states, "At autopsy, one cannot specifically tell from the extent of the injury if an individual has been shot by a .38 Special 158 gr RN [round nose] lead bullet traveling at 789 ft/s or a 110 gr Norma HP [hollow point] at 1334 ft/s" [4]. This statement leads one to conclude that at handgun bullet velocities, the final wound track shape is fairly constant for all bullet constructions. This conclusion is further supported by the work of Dr. Harrell, a member of the Board of Police and Fire Surgeons, and the final "wound track" observed in numerous gelatin targets. However, x-ray studies of bullets interacting with animal tissue and high speed studies of bullets interacting with gelatin targets clearly show that different bullet constructions do have different temporary effects on the target medium. To deal with this situation, a measure of bullet performance, called the Maximum Temporary Cavity (MTC), has been developed.

The Maximum Temporary Cavity, simply defined, is the curve connecting the points of maximum temporary displacement of the target medium around the bullet track. Since the volume of the MTC changes with bullet construction and bullet velocity while the final wound channel may not, the volume of the MTC was chosen to be the measure of bullet performance for this study.

Over the years many different target simulant materials have been proposed and used (animals, clay, soap, sand, wet paper, gelatin, etc.) and different researchers tend to have their own favorites. The usual reasons for choosing a particular simulant are cost, availability, ease of use, and the researcher's familiarity with the material's performance relative to the real world. In this study a tissue simulant meeting the following criteria was sought:

1. The material must provide reproducible results.
2. The material must behave similar to tissue when struck by a bullet.
3. The material should have a sufficient history so that comparisons to the historical work can be made.

As a result of wound ballistics experiments in the 1940's and 1950's it became well known that trauma such as bone fracture, hemorrhage and nerve damage could occur beyond the permanent wound track of complete tissue maceration. By 1962, when the U.S. Office of the Surgeon General published a treatise on wound ballistics, the kinetic energy mechanism of wounding was accepted to be cavitation. The basic idea is that as the bullet penetrates soft tissue it cuts and tears tissue directly in its path. In addition, the bullet transfers some of its momentum to the neighboring tissue causing an outward radial motion. This outward motion can be thought of as rings of tissue expanding about the bullet path. Often this expansion severely stretches or tears the tissue and trauma results. Experimental evidence has shown that the rate at which bullets transfer momentum to the surrounding tissue as a function of penetration distance is very similar to that observed in gelatin.

Therefore, the material chosen as the tissue simulant for this study was 20 percent gelatin at a temperature between 8 and 10 °C (46.4 and 50 °F). The choice of 20 percent gelatin as the target material rather than another simulant is based on the following considerations:

1. Similarity between bullet retardation in gelatin and animal tissue.
2. Similarity between the size and shape of the temporary cavity in gelatin and tissue. Figure 8 depicts the results of measuring the temporary cavities produced when a steel sphere impacts the two test media (pig muscle and gelatin) at essentially the same velocity.
3. Similarity between the permanent cavity remaining in tissue and gelatin after the passage of a bullet.
4. Homogeneity/reproducibility of the gelatin response to bullet penetration.
5. The material has been in use since the 1940's for wound ballistics experiments, yielding a reasonable amount of historical data for comparisons.

The exact formulation and mixing directions for the gelatin used for the test firings described in this report are fully described in Police Handgun Ammunition, Volume II [9]. In general, a mixture of 20 percent gelatin and 80 percent hot water (by weight) is poured into containers approximately 15×15×30 cm (5.9×5.9×11.8 in). After debubbling, the containerized mixture

is placed in a cooler and allowed to jell. Once solidified the blocks of gelatin are removed from their containers and stored at a temperature between 8 and 10 °C (46.4 and 50 °F) until just before they are used.

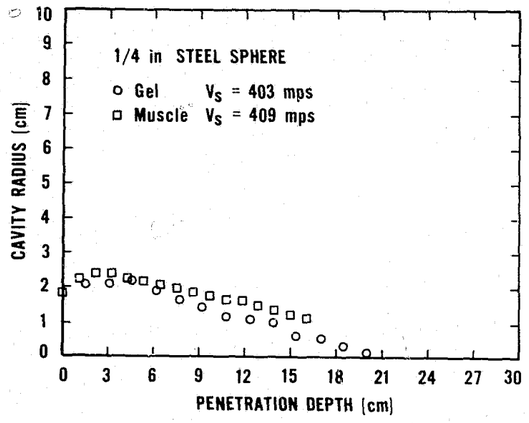

FIGURE 8. *Comparison of the maximum temporary cavity for a steel sphere penetrating animal tissue and tissue simulant.*

Maximum Temporary Cavity Data

Commercially available bullets in the diameter range 9 mm (355 caliber) to 45 caliber were fired at various velocities into gelatin test blocks and the results photographed to obtain the MTC. Figure 9 shows a typical result for a full metal jacket bullet impacting gelatin when the photographic movie frames are traced one on top of each other. The MTC is the outer boundary of such a composite tracing. Plots of the MTC for the bullets tested as part of this study are presented in the experimental data report [9].

The ammunition used consisted primarily of hand-loaded cartridges. Bullet velocities were adjusted such that striking velocities varied nominally between 120 m/s (400 ft/s) and 700 m/s (2300 ft/s). Most weights and types of bullets either available from or supplied by the commercial manufacturers were evaluated. The manufacturers were chosen such that the vast majority of bullets used in commercial handgun cartridges could be evaluated. The actual bullets tested came from the following manufacturers:

Hi-Precision	Smith & Wesson
Hornady	Speer
MB Associates	Super Vel
Remington-Peters	Winchester-Western
Sierra	Zero

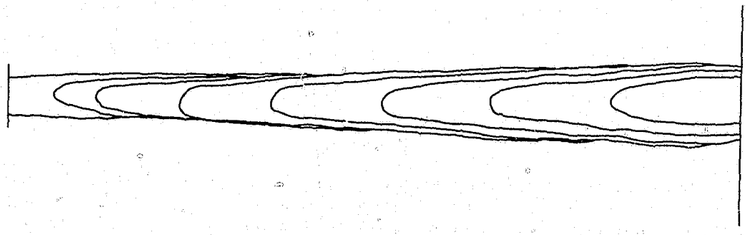

FIGURE 9. *Time histogram of the gelatin displacement when impacted by a full metal jacket bullet.*

For the gelatin firings, special "Mann barrels" were used. Since one of the more important parameters under investigation was the effect of bullet velocity on the ranking index, it was necessary to examine velocity levels below and well above those experienced with standard cartridges fired from standard weapons. In the case of high and low velocity testing, chamber pressures can exceed those permissible in standard handguns. Thus, for safety reasons Mann test barrels were used. *At this point it should be noted that even though RII results were examined up to velocities approaching 700 m/s (2300 ft/s), the powder charges necessary to attain these velocities from standard handguns may produce chamber pressures well above acceptable safety limits. Further, light powder charges can also produce chamber pressures above acceptable safety limits.*

The justification for testing at nonstandard velocities and chamber pressures was manifold. It is well documented in previous studies by many investigators, that different type bullets deform differently as a function of impact velocity. It was the purpose of this study to develop a general criterion. This requires that RII be known as a continuous function of velocity. To this end, it was important to know the degree of degradation experienced in RII if lower than standard velocities are used, i.e., velocities below the bullet deformation velocity. Also it was important to determine if the effects of possible excess deformation or fragmentation of the bullet at higher than standard velocities enhance or degrade the ranking index. If only commercial loadings were used and the ranking index was reported for just these particular cartridges, future changes in loading specifications by a manufacturer to alter velocity would make the ranking of limited usefulness.

The experimental setup is depicted schematically in figure 10. The bullet passes through a series of chronograph screens that are used to start and stop the velocity measurement system and then into the gelatin target. A high-speed movie camera, located at right angles to the line-of-fire, photographs the performance of the projectile in the target at 10,000 frames/s (one picture every 0.0001 s). These movies represent the raw data for the MTC measurements undertaken for this study.

Based on the work of Dubin [10] it is possible to mathematically predict the dimensions of the MTC in gelatin produced by certain types of projectiles. Appendix C presents the mathematical derivation of such a mathematical equation and the empirically-derived constants required to use the model. The model is valid for rigid nontumbling projectiles. Rigid projectiles include most jacketed bullets and (by experimental observation) lead bullets with striking velocities less than 240 m/s (787 ft/s).

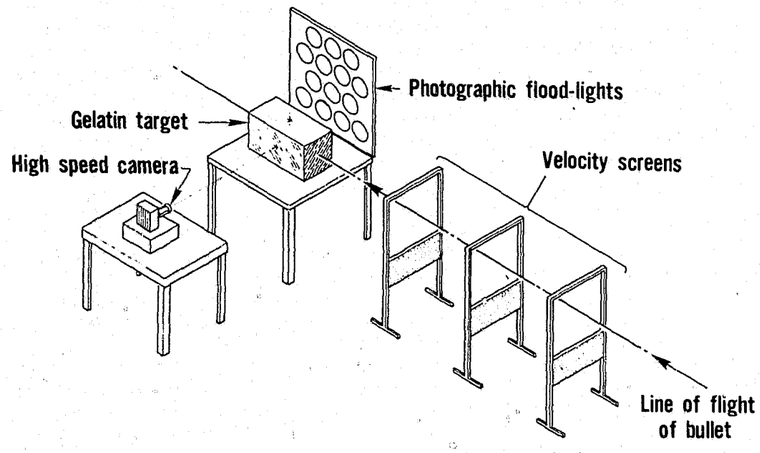

FIGURE 10. *A schematic representation of the experimental test setup.*

In this report the theoretical cavity model was used to provide predicted cavity data for selected projectiles, primarily those projectiles that did not deform at the commercially-loaded velocity. The cavities predicted using the model provided data points at low velocity values so that average RII vs. velocity curves could be drawn for those projectiles where one or two shots at or

above commercial velocity were sufficient to indicate that the collection of a full set of data for the bullet was not warranted.

RELATIVE INCAPACITATION INDEX (RII)

The basic elements can now be combined to produce a single number to rank each bullet as a function of shooter capabilities, human target characteristics, and the physical parameters of the bullet. The V. Ind. function is a set of numbers that represents the relative vulnerability at each depth of bullet penetration of the human body taking into account the construction of the body, the achieved marksmanship of trained shooters shooting in a stressful situation and using a weapon/ammunition combination giving medium to heavy recoil (not 44 magnum level recoils), and the average engagement range of 6 m (19.7 ft). The dimensions of the MTC are a set of numbers that provide a measure of performance of the bullet in a soft target medium as a function of caliber, bullet construction, and striking velocity. To combine all of these conditions together, the volume of the MTC for each unit of bullet penetration (for this study the unit of depth was chosen to be "one centimeter") is multiplied by the vulnerability index at that depth and each weighted volume is added to all the other weighted volumes to obtain a single number. A practical example of how this is done is presented in the "sample calculations" section of this report.

Data Reduction and Analysis

Over the long period of this study a large volume of MTC data was amassed. For convenience of analysis the data were stored in a computer file. Computer programs were written to perform various calculations such as RII from the MTC data, to plot RII vs. velocity curves for a particular bullet type, to plot cavity data, to predict the maximum temporary cavity for rigid nontumbling projectiles, etc.

The types of data stored included projectile manufacturer, caliber, mass and construction type (such as jacketed soft point, lead round nose, etc), the experimental cavity dimensions, and striking velocity.

As is demonstrated in the example section, given the MTC dimensions and the tabulated values for the V. Ind., the RII for that round can be calculated using a hand or desk calculator. However, obtaining the cavity dimensions experimentally does require special equipment.

It should be noted that for all of the data analysis performed for this study, the symmetrized cavity envelope contour as measured from high-speed movies was used. The cavity measurements were taken at approximately 5-mm (0.2 in) increments of penetration. The phrase "symmetrized cavity envelope" means the array of depths of penetration and maximum cavity radii for each depth measured. The radii are taken to be one-half of the cavity dimension which is perpendicular to the projectile path. This symmetrization procedure is justified on the basis of numerous observations. For example, in 1957, M. Kraus published x-ray pictures of temporary cavities in animal tissue showing nearly circular transverse cross sections [11]. This is not to imply that the *permanent* wound channel is circular in cross section. The reason temporary cavities are nearly circular in cross section is due to the principle of minimization of energy for any physical system, vis. the cavity boundary seeks a configuration of minimum surface area. Furthermore, although neither the longitudinal nor transverse cross sections for any particular cavity are exactly symmetric, the variations from symmetry occur in the nature of statistical fluctuations, and no significant trend was observed in the data gathered for this study.

The data were also analyzed for trends in RII vs. bullet weight for various calibers, RII vs. bullet construction and shape, general maximum cavity shape/size vs. projectile velocity, and curve shape for RII vs. velocity for each projectile construction type. The results for all except the RII vs. velocity study are presented in the conclusion section. Because of its importance, the RII vs. velocity study is presented next.

For each bullet fired into a gelatin test target, the RII value was calculated using a computerized version of the procedure presented in the example section. For a given bullet type (e.g., 38 caliber; 158 grain; jacketed hollow point; manufactured by Hornady, Remington, Smith & Wesson, and Winchester-Western) the RII's achieved by actually firing the projectile into gelatin were plotted vs. velocity. When large numbers of these curves are examined together trends are observed.

The data divide into three trend areas as a function of velocity. The transition zones are different for different bullet constructions and are not extremely distinct for any of them. For discussion purposes, we will call the three areas: low velocity, working velocity, and high velocity.

RII vs. velocity for low velocity values must start at zero for all projectiles for obvious reasons. As velocity increases, so does RII; however, in the low velocity part of the curve, RII increases slowly as velocity increases and the projectiles exhibit either very little or no deformation. This is the region in which the theoretical cavity model is valid. As with any experimental data, there is scatter. However, the data can be approximated by a straight line rising with slope α_1 starting at the graph origin.

In the working velocity region, RII increased much faster with increasing velocity. Within this region, bullet upset or deformation readily occurs. The MTC's have substantial volumes extending from 0 to at least 22 cm into the gelatin target. The data are again scattered; however, the data can be approximated by a straight line with slope α_2; generally much greater than α_1. It should be noted that much of the experimental data gathered for this study terminate in this region because chamber pressures to achieve higher velocity were well above the allowable commercial chamber pressure.

At higher velocities, RII decreases with increasing velocity; the cavity in the gelatin gets larger in diameter, but shorter in length. Since RII is tied to the vulnerability of the human body, this reflects a projectile that does not penetrate sufficiently to interact with the tissue deeper in the body. In the high velocity region, the data can again be approximated by a straight line with a negative slope α_3.

The three regions described above are depicted in figure 11. Figure 12 shows the plots of the MTC for the Winchester-Western 85 grain jacketed hollow point as taken from the raw data for five different velocities. Above each MTC is presented the round identification number, the RII (calculated from the MTC and the average vulnerability index) in square brackets, the striking velocity in meters per second, and the striking velocity in feet per second. This series of plots clearly shows the overall trend. At low velocity [189 and 225 m/s (621 and 740 ft/s)] , there is little bullet deformation and the MTC's are narrow and deep. At working velocities of 300 m/s (986 ft/s), the factory load, and 320 m/s (1049 ft/s), the MTC has reasonable diameter and penetrates to approximately 15 cm (5.9 in). At high velocity, 374 m/s (1226 ft/s), the diameter of the MTC increases but the penetration decreases. If the bullets were fired at higher impact velocities, ultimately the RII would decrease. In this example the velocity was not taken high enough to measure the slope of the decreasing portion of the curve since the chamber pressure to achieve 374 m/s (1226 ft/s) was already well above the industry specification for the 380 Auto round being tested.

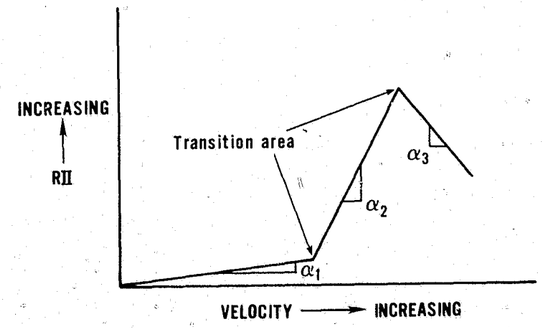

FIGURE 11. *Idealized general RII vs. velocity curve.*

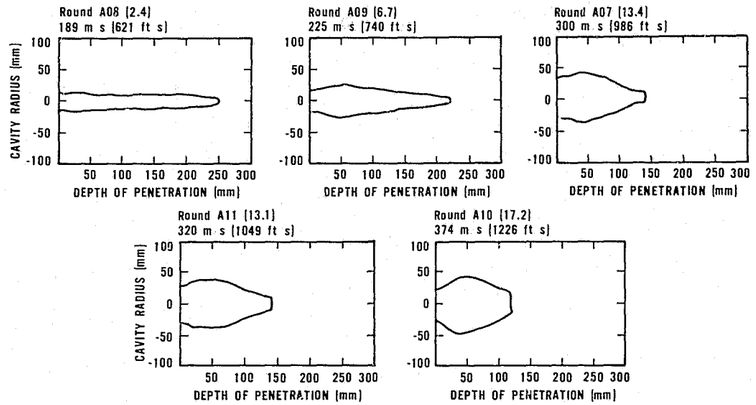

FIGURE 12. *Maximum Temporary Cavity (MTC) plots for the Winchester-Western, 85 grain, jacketed hollow point, 9 mm.*

RII Predictive Equation

The final consideration for this study was to create a simple method for estimating RII for bullets of interest based on simple measurements. Such a method was established and is based on standard curve fitting procedures. A curve was chosen that fits the general nature of the data just described, then the curve constants were adjusted so that a best fit to the data points was obtained. In some cases the values of the curve fitting parameters are based on limited data and the true values of these parameters could differ noticeably from the values given. Knowing the curve constants for a bullet of interest, the velocity at which the bullet will strike the target, and a minor correction factor based on who manufactured the bullet allows, through the use of the predictive equation, prediction of the bullet's RII. The only measurement required is the achieved bullet velocity for the cartridge/weapon combination.

An equation that smoothly fits the RII vs. velocity data collected during this study is:

$$RII = e^{(A+BV+C/V)} + \text{Average Deviation}$$

where

e is the natural logarithmic base 2.71828;
A, B, and C are curve constants that are projectile dependent; and
V is the striking velocity.

The average deviation is the amount plus or minus that a given manufacturer's product deviates on the average from the predictive curve for a given projectile.

Figure 13 is an actual RII vs. velocity curve taken from the raw data. For clarity, only the solid part of the curve is presented in the raw data report. The dotted line at the low velocity end is where the curve would go if the data were extended in that direction. In the absence of actual firing data, it is not possible to predict the exact slope of the curve at the high velocity end, but the dotted line indicates the general shape of the curve. In appendix B where the values of A, B, and C are tabulated, the maximum test velocity is also stated. The predictive equation is not expected to produce good results for bullet velocities above the maximum test velocity or near zero velocity.

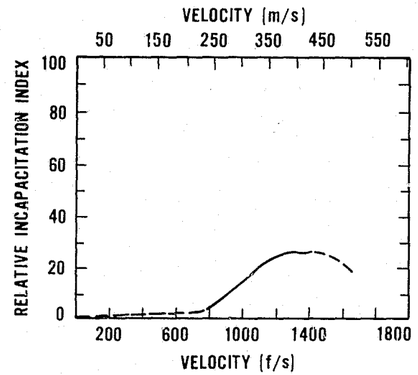

FIGURE 13. *Relative incapacitation index as a function of velocity for 95 gr, JHP (Silvertip), 38 caliber bullet manufactured by Winchester-Western.*

Commercial Ammunition Data

The next task was to rank commercial ammunition. Boxes of commercially-loaded ammunition were purchased "off-the-shelf" from local gun dealers. The cartridges were fired from representative handguns to obtain an average achieved velocity. There were several reasons why such a firing was necessary.

1. At the time this study was conducted, the use of vented test barrels (to simulate revolver performance) was not widespread or at least the results were not reported to the public.
2. The industry-approved method for making chamber pressure and bullet velocity measurements did not match the actual usage of the cartridges.
3. The first firing series was only designed to evaluate the performance of the bullets and a necessary objective of the program was to evaluate the available commercial cartridges.

The firing of commercially-loaded cartridges in representative handguns was performed with the same setup as is shown in figure 10. However, only velocity data were gathered. The measured velocity data reported in the Executive Summary in table 1 is an average for 10 shots. Cartridges from the following manufacturers were included in this firing:

Browning	Speer
Federal	Super Vel
Remington-Peters	Winchester-Western
Smith & Wesson	3-D

SAMPLE RII CALCULATIONS

From MTC Data

To calculate RII each small increment of cavity volume is multiplied by the V. Ind. value at the corresponding depth of penetration. The sum of these weighted volume increments is the RII and is given by the following formula:

$$RII = \sum_{x=1}^{x=\text{Max Penetration}} \pi r^2(x)\ [\text{V. Ind. }(x)]$$

where

$\pi = 3.14$
$r(x) =$ the radius of the symmetrized cavity at depth x.
V. Ind.$(x) =$ the value of the V. Ind. at depth x.

For information, and as an example of how to calculate RII "by hand," table 3 presents a sample RII calculation from MTC data. The round used as an example is a Winchester-Western, 230 grain, 45 caliber, full jacketed bullet impacting the gelatin target at 244 m/s (801 ft/s), the round identification number is A22 and a plot of this cavity is shown as figure 14. From table 3, the measured RII value is 7.3. This value of RII for the venerable 45 ACP round is supported by round number A23, the Remington, 230 grain, full jacketed bullet that had a striking velocity of 263 m/s (864 ft/s) and an RII of 8.3. It should be noted that measured RII's are calculated using metric units, however, when RII's are predicted using the predictive equation, the curve fitting parameters have been calculated such that velocity in feet per second should be used.

TABLE 3.

Penetration depth (cm)	Vulnerability index (V. Ind.)	Cavity radius r(cm)	r^2(V. Ind.)
1	0.0061	1.8	0.020
2	0.0169	1.8	0.055
3	0.0477	2.1	0.210
4	0.0608	2.0	0.243
5	0.0588	2.0	0.235
6	0.0564	2.0	0.226
7	0.0458	1.9	0.165
8	0.0388	2.0	0.155
9	0.0401	1.9	0.145
10	0.0405	1.9	0.146
11	0.0248	1.9	0.090
12	0.0238	1.8	0.077
13	0.0292	1.7	0.084
14	0.0231	1.7	0.067
15	0.0227	1.8	0.074
16	0.0273	1.5	0.061
17	0.0230	1.9	0.083
18	0.0247	1.9	0.089
19	0.0196	1.9	0.071
20	0.0074	1.9	0.027
21	0.0014	1.8	0.005
22	0.0003	2.0	0.001

Total = 2.329

RII = π Total = 3.14 × 2.329 = 7.3

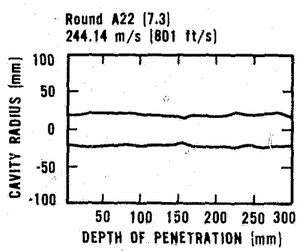

FIGURE 14. *Plot of Maximum Temporary Cavity for a 230 grain Winchester-Western full metal jacket bullet impacting gelatin at 801 ft/s.*

From the Predictive Equation

To predict an RII for a given cartridge, the following procedure should be used:

1. Measure the actual muzzle velocity in feet per second (ft/s) fired from the intended service weapon (the average velocity for a series of 10 shots is recommended).
2. Specify the bullet (not cartridge) type by:
   a. manufacturer (this may not be identical to the cartridge manufacturer);
   b. construction, i.e., LRN, JHP, SWC, etc.;
   c. mass in grains; and
   d. caliber.
3. Locate the appropriate table in appendix B starting with the manufacturer of the bullet.
4. Use the values of A, B, and C found in the table in the following equation:

$$\overline{RII} = [\exp(A+BV+C/V)] + \text{Average Deviation}$$

where

A, B, and C are the coefficients tabulated in appendix B;
V is in feet per second; and
Average Deviation is in units of RII.

To illustrate this procedure, the prediction of RII for test bullet number A22 (the projectile for which the RII is calculated from MTC measurements in the example of table 3) is as follows:

1. Muzzle velocity: 801 ft/s
2. a. Winchester-Western
   b. Full jacket
   c. 230 grains
   d. 45 caliber
3. Using table B9 (see appendix B) for the Winchester-Western, 45 caliber, 230 grains, FMJ, at 1164 ft/s or less.

A = -4.44360010E-03*
B = 2.77197163E-03
C = -536.5915478282

Average Deviation = -1.12

4. Then to calculate the predicted RII: $(A+BV+C/V) = (-4.44360010\times10^{-3}) + (2.77197163\times10^{-3}\times801) + (-536.5915478282)/801 = 1.546003619$

RII = exp(A+BV+C/V) + Average Deviation
RII = exp(1.546003619) - 1.12
RII = 4.692678926 - 1.12
RII = 3.6

The predictive equation was developed to provide a means of estimating the RII of a bullet without the expense of controlled experiments to measure the MTC. It is useful as a screening method to compare the expected performance of one bullet relative to another, but is not a substitute for MTC determinations. Test data for round A22 were intentionally selected for use in the preceding example RII calculations. While the predicted RII of 3.6 is considerably less than that based on MTC measurement, 7.3, either value would lead one to conclude that the bullet is a poor choice for a service round. With regard to the accuracy of the RII estimated by use of the predictive equation, one must recognize that the coefficients presented in appendix B are greatly influenced by the number of data points that were used to determine the relationship of RII as a function of velocity for a specific bullet. This research concentrated the experimental effort on the most commonly used service rounds, i.e., 38 caliber bullets.

The coefficients presented in appendix B for bullets in common usage, when used with the predictive equation will in general provide estimates of RII that are in good agreement with those obtained from MTC measurement. For example, the predicted RII of bullet number A07 at a

*For coefficients with a magnitude less than 1.0, scientific notation is used with the base being the number 10. For example "A" above is read as -4.44360010×10^{-3} or as -0.004443601. The symbol "E" is used to indicate the power of 10 required to put the number into the correct order of magnitude.

velocity of 300 m/s (986 f/s) is 13.5, while that obtained from MTC measurement is 13.4. In the case of round A02, at a velocity of 325 m/s (1067 f/s) the two methods yield an identical RII of 18.0. An analysis of variance, to establish error bands for the predictive equation by bullet types has not been made. Undoubtedly, future research will seek to establish the limits of the predictive equation, and to refine the coefficients to improve the accuracy of the estimated RII. In the meantime, the predictive equation can be used as a means of comparing the relative performance of bullets considered for service use. If the RII must be precisely determined, it remains essential to obtain a measured MTC through a gelatin block test, and to calculate the RII as was done in table 3.

The data presented in table 1 at the end of the Executive Summary presents the RII for commercial handgun cartridges calculated using the above predictive procedure. These data have been in circulation in several different forms since 1975. Over the years as new data became available and as calculation procedures were refined, certain of the RII numbers have changed from one version of the table to later versions.

There will always be pet bullets and/or pet loadings that place lower in the rankings than expected. There will also be some sleepers that place higher in the rankings than expected. It must be remembered that the ranking (i.e., RII value) is the result of the evaluation criterion chosen. As more data are gathered, as more sophisticated evaluation criteria are developed, as field performance data are amassed, and as manufacturers change their loadings, the cartridge rankings can be expected to change.

CONCLUSIONS

Bullet Velocity

In the range of calibers studied, the most important property of a moving handgun bullet affecting its performance in the target medium is its striking velocity.

First, the size of the Maximum Temporary Cavity (MTC) depends partly on the striking velocity, i.e., the volume of the MTC depends on the total energy available.

Second, there is a threshold velocity, below which a given bullet will not deform; deformation of the bullet greatly affects the size and shape of the MTC.

It should be stressed, however, that one cannot use the striking kinetic energy as the sole criterion for ranking handgun bullets. It is the size and shape of the resulting MTC and how it effects the body that ultimately gives one bullet a higher RII than another. Some lighter bullets yield a higher RII than heavier ones having the same striking kinetic energy, shape, construction and caliber. From RII and penetration considerations, a velocity of approximately 335 m/s (1100 ft/s) appears most effective. At this velocity, deformable bullets expand sufficiently in soft tissue to provide effective RII's without overpenetrating the target.

Caliber

The caliber of a bullet, together with its shape, establish the initial value of its presented area. It is this area of the interface between the bullet and the target medium that enters the formula for the envelope of the MTC; the sectional area of the bullet (proportional to the caliber squared) cannot be used once the bullet begins to deform. Thus, a larger caliber bullet will yield a higher RII at nondeforming velocities; once deformation is possible, smaller caliber bullets may outperform larger calibers. The 45 caliber bullet offers the greatest growth potential of the calibers tested. This is not surprising since the initial diameter of the 45 caliber bullet is as large as some of the deformed small caliber bullets' final diameter. Proper design of the 45 caliber bullet to enhance deformation could result in these bullets outperforming the smaller calibers. It should be remembered that at the time that the commercial ammunition was shot for table 1, deforming 45 caliber bullets were not in general usage.

Bullet Mass

The mass of the bullet affects the size and shape of the MTC. A lighter bullet will slow down more rapidly in the target medium and a heavier bullet will penetrate further; this affects the

location of the maximum radius of the MTC. In this case, it is the penetration depth of the temporary cavity with respect to the depth of vulnerable tissue that produces varying degrees of RII. However, for law enforcement purposes it is considered undesirable for bullets to go completely through a human target and thereby pose a hazard to bystanders. The data show that bullet masses in the range of 158–170 grains seem to perform within the guidelines of good RII without overpenetration.

Bullet Shape

The effect of bullet shape (bluntness of the nose) is important only in that it establishes the initial value of the hydrodynamic drag coefficient. This coefficient enters the formula for the envelope of the MTC and it is also a part of the formula for the threshold deformation velocity. At velocities too low for deformation to occur, the hydrodynamic drag coefficient is a constant and the effect is that blunter bullets yield higher values of RII.

At velocities sufficient to cause deformation of the bullet, the hydrodynamic drag coefficient changes as the bullet deforms. Bullets with smaller initial values of drag coefficient can deform in such a way as to outperform those with a higher initial drag coefficient.

Deformation and Bullet Construction

Deformation of a handgun bullet depends strongly on both velocity and construction. Construction involves principally whether the bullet is jacketed or not; the length, thickness; and hardness of the jacket material; the presence of hollow nose cavities, the presence of hollow bases; and the hardness of the core material. Construction also directly affects fragmentation of the bullet in both hard and soft targets.

In order to study the effect of construction on RII, a plot of RII vs. velocity for different bullet constructions in 357 caliber was made. This composite plot is shown as figure 15. It is

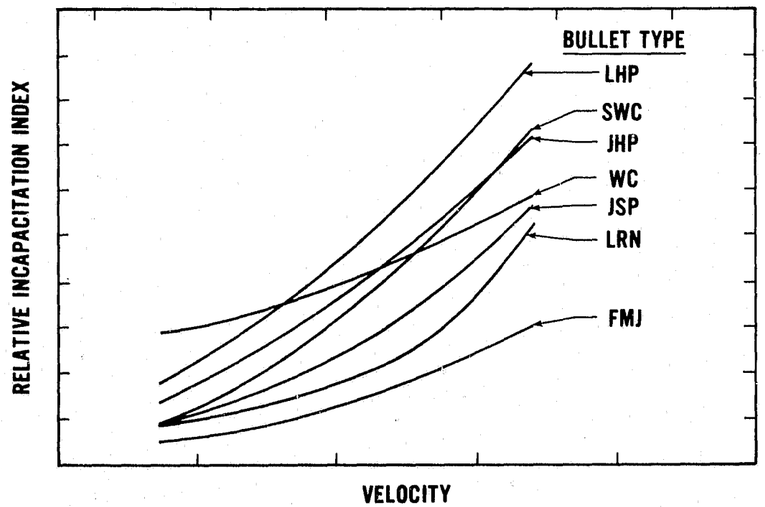

FIGURE 15. *RII vs. velocity with bullet construction as an independent parameter.*

clearly seen from figure 15 that the general ranking of bullet construction in order of decreasing RII performance is:

Best

a. Soft lead hollow points (LHP)
b. Jacketed hollow point (JHP)
c. Semi-wadcutter (SWC)
d. Wadcutter (WC)
e. Jacketed soft point (JSP)
f. Lead round nose (LRN)
g. Full metal jacketed (FMJ)

Poorest

With the exception of the full-metal-jacketed bullet, the onset of deformation occurs at a given velocity for each bullet construction type and hardness (a–f); i.e., hollow-point bullets begin deforming at a velocity above 215 m/s (705 ft/s) and lead round nose bullets begin deforming at velocities above 340 m/s (1115 ft/s). Unless the bullet's striking velocity exceeds these threshold values, bullet deformation is highly unlikely. Note that these threshold velocities were obtained by flash x-ray photography; they cannot be obtained by an inspection of the RII vs. velocity curves, although they are consistent with the curves developed as part of this study. As discussed in the evaluation criterion section below, the authors recommend the use of deforming bullets by law enforcement personnel.

Shooter Accuracy

The RII increases as shooter accuracy increases. However, the effect of handgun type/cartridge combinations on shooter accuracy has not been fully addressed in this study; it is the subject of possible future work.

Point of Aim

The RII is dependent on the aim point chosen. Assuming a given degree of shooter accuracy, the data indicates that an aim point slightly higher (armpit level) than that used on standard silhouette targets increases the probability of incapacitating a human target. See appendix D for a detailed discussion of this issue.

Evaluation Criterion—RII

The RII is a valid evaluation criterion for cartridges intended for handgun usage. It explicitly measures the performance of projectiles in a simulant for soft tissue. It implicitly includes within its weighting function, tissue interfaces, vital organ placement, shooter accuracy under stress conditions, and the main objective of handgun usage (the stopping of further aggression rather than simple lethality).

The RII is not the only valuable evaluation criterion nor is it the last word in such criteria. There is extensive work remaining to be done on the description and modeling of the physiological effects of projectiles on animal targets including humans. Further, work could be done on the interaction between stress, perceived recoil, and shooter accuracy.

Finally, a word on how much RII is best. It is the opinion of the authors that RII's of less than 10 are representative of bullets that produce low-volume maximum temporary cavities; therefore, the probability of the MTC affecting vital tissue is low. It would then appear that the higher the RII the better. It was observed in this study that nondeforming bullets can achieve respectable RII's if they have relatively high velocity. However, the same performance can be achieved with deforming bullets at lower velocities. Further, high velocity nondeforming bullets rarely expended all of their energy in the target while deforming bullets usually stayed within the target material, thereby presenting less of a hazard to bystanders. Again, it is the observation of the authors that deforming projectiles with RII's 30 and below generally did not overpenetrate the target while giving reasonable size MTC's.

There is no ideal firearm system (weapon/ammunition) for all situations. Each law enforcement department must evaluate its own special requirements and choose a defensive

weapon system capable of meeting its needs. However, this study has shown that for handguns in the 9 mm/38 caliber to 45 caliber range, a deforming projectile, driven at a velocity above the minimum deformation velocity, and an RII between 10 and 30 is a reasonable goal for handgun ammunition for use against normally clad assailants in an urban environment.

APPENDIX A—REFERENCES

[1] Dobbyn, R. C.; Bruchey, W. J., Jr.; Shubin, L. D. An evaluation of police handgun ammunition: Summary report. National Institute of Justice; 1975 October; LESP-RPT-0101.01.

[2] Hatcher, J. S. Textbook of firearms investigation, identification, and evidence. Small Arms Technical Publishing Company; 1935.

[3] Sturdivan, L., et al. Terminal behavior of the 5.56 mm ball bullet in soft targets. Ballistic Research Laboratory; 1969 August; Report 1447.

[4] DeMaio, V. J. M., et al. Comparison of wounding effects of commercially available ammunition suitable for police use. FBI Law Enforecment Bulletin. 43(12); 1974.

[5] Private communication from James Torre, U.S. Army Human Engineering Laboratory, to William J. Bruchey, Jr., U.S. Army Ballistic Research Laboratory. The data is also available from a report prepared by Jezek, Bruce, "Personal defense weapons (PDW) summary report." U.S. Army Small Arms Systems Agency; 1972 May; Confidential Report ADC010750.

[6] H. P. White Laboratory. Basic and time-stress tests of caliber 38 special (LEAA). U.S. Army Land Warfare Laboratory; 1973 January; Technical Note 73-01.

[7] Stanley, C. H.; Brown, M. A computer man model. Ballistic Research Laboratory; 1978 May; Report ARBRL-TR-02070.

[8] U.S. Army Contract DAAD05-75-6-0730.

[9] Bruchey, W. J.; Frank, D. E. Police handgun ammunition: Incapacitation effects. Volume II: Experimental data. National Institute of Justice; Report 101-83.

[10] Dubin, H. C. A cavitation model for kinetic energy projectiles penetrating gelatin. Ballistic Research Laboratory; 1974 December; Memorandum Report No. 2423.

[11] Kraus, M. Studies in wound ballistics: Temporary cavity effects in soft tissue. Medicine. 121: 221–231; 1957.

APPENDIX B—TABLES OF COEFFICIENTS FOR THE RII PREDICTIVE EQUATION*

*Note: The equation, "exp(A+BV+C/V) + Average Deviation," used in this report was chosen because it can by proper choice of A, B, and C, produce curves having shapes that qualitatively match those deemed reasonable. No assessment of the statistical significance of the parameters has been done. In order to assess the statistical significance of the parameters, a new program aimed at gathering large quantities of data on a limited number of bullet types would be required. Reference 9 presents that data gathered in this study as well as the curves generated by the A, B, and C's presented in this appendix. Abbreviations used in tables B1 through B10: PTS—Points; %Pos.—Percent of points that are above the curve.

TABLE B1. *Hi-Precision*

Caliber	Weight (grains)	Type	Maximum test velocity (feet/second)	A	B	C	Average deviation	PTS	% pos.
38	110	JHP	1725	2.685827088166	1.48286991E-03	-1639.961723535	-4.06	6	0.00
38	158	JSP	1761	2.284496287811	1.79523251E-03	-1626.224818408	-6.59	4	0.00
44	240	JHP	1210	6.420674639184	-1.93650849E-05	-3121.181150618	0.06	4	50.00
45	170	Hemi/JHP	1279	-4.75961025E-03	3.52057612E-03	-753.9400377023	-0.57	3	66.66

TABLE B2. *Hornady*

Caliber	Weight (grains)	Type	Maximum test velocity (feet/second)	A	B	C	Average deviation	PTS	% pos.
38	110	JHP	1725	2.685827088166	1.48286991E-03	-1639.961723535	-0.91	11	27.27
38	125	JHP	1837	4.268997195447	8.61674999E-04	-2512.299363429	-0.59	9	44.44
38	158	JHP	1748	5.463778587451	2.41878706E-04	-2826.097748446	0.44	7	57.14
38	158	JSP	1761	2.284496287811	1.79523251E-03	-1626.224818408	4.07	6	66.66
41	210	JHP	1164	-1.76702518E-02	3.66871359E-03	-658.0391049244	5.28	5	80.00
44	200	JHP	1240	3.666153538256	1.69946042E-03	-2163.581009684	-2.90	6	0.00
44	240	JHP	1210	6.420674639184	-1.93650849E-05	-3121.181150618	0.00	5	60.00

TABLE B3. *MB Associates*

Caliber	Weight (grains)	Type	Maximum test velocity (feet/second)	A	B	C	Average deviation	PTS	% pos.
38	63.9	SS	1053	-30.82212498421	2.34343443E-02	9525.324936997	0.00	3	66.66

TABLE B4. *Remington*

Caliber	Weight (grains)	Type	Maximum test velocity (feet/second)	A	B	C	Average deviation	PTS	% pos.
9 mm	115	JHP	1512	0.441116438577	2.86405759E–03	–797.6466613514	3.98	6	83.33
9 mm	124	FMJ	1394	1.36866961E–03	3.03046062E–03	–964.1634308418	0.32	4	75.00
38	95	JHP	1397	17.66599655536	–4.92163066E–03	–10042.07959894	0.00	4	50.00
38	125	JHP	1837	4.268997195447	8.61674999E–04	–2512.299363429	3.96	18	50.00
38	148	WC	1794	1.260402154507	1.52503957E–03	186.5770158893	1.89	3	66.66
38	158	JHP	1748	5.463778587451	2.41878706E–04	–2826.097748446	2.83	3	33.33
38	158	JSP	1761	2.284496287811	1.79523251E–03	–1626.224818408	0.50	3	33.33
38	158	LRN	1266	–5.033894694484	5.26967465E–03	1916.501103882	1.74	5	40.00
38	158	MP	1578	–2.11528401E–03	2.77168214E–03	–993.161798543	–2.06	3	0.00
38	158	SWC	1719	6.729291308774	–7.33217328E–05	–3918.064161714	–3.76	3	0.00
38	185	JHP	1161	4.03287990E–04	3.75260300E–03	–898.7414499336	0.16	1	100.00
38	200	LRN	1302	–4.06476920E–03	2.92772680E–03	–517.4344982668	–0.04	3	33.33
41	210	JSP	1276	–22.62956492331	1.40939623E–02	11104.99248834	0.08	5	60.00
41	210	SWC	1430	6.168620175805	1.28604390E–03	–5252.00040152	0.00	4	50.00
45	185	JHP	1180	17.87498265475	–5.17721571E–03	–9269.667489503	0.08	7	28.57
45	185	WC	1230	–2.64198664E–02	2.79817047E–03	–175.5762192963	–4.34	1	0.00
45	230	FMJ	1243	–2.79182674E–03	2.92603370E–03	–615.0977736153	–1.81	1	0.00

TABLE B5. *Sierra*

Caliber	Weight (grains)	Type	Maximum test velocity (feet/second)	A	B	C	Average deviation	PTS	% pos.
38	110	JHP	1725	2.685827088166	1.48286991E-03	-1639.961723535	-1.50	7	28.57
38	125	JHP	1837	4.268997195447	8.61674999E-04	-2512.299363429	-2.33	6	33.33
38	125	JSP	1407	3.833194355271	9.99823834E-04	-2303.088990996	-2.76	7	14.28
38	150	JHP	1335	3.384355727232	1.40351211E-03	-2137.976826352	0.47	6	66.66
38	158	JSP	1761	2.284496287811	1.79523251E-03	-1626.224818408	-1.85	7	28.57
41	170	JHP	1164	-1.63011812E-03	2.80051558E-03	-489.946793937	-0.31	1	0.00
41	210	JHP	1164	-1.76702518E-02	3.66871359E-03	-658.0391049244	-21.13	1	0.00
44	180	JHP	1217	-2.49956217E-03	2.55065907E-03	-353.3126889531	-0.40	1	0.00
44	240	JHP	1210	6.420674639184	-1.93650849E-05	-3121.181150618	-29.65	1	0.00

TABLE B6. *Smith & Wesson*

Caliber	Weight (grains)	Type	Maximum test velocity (feet/second)	A	B	C	Average deviation	PTS	% pos.
9 mm	90	JSP	1558	-3.20687575804	3.84511448E-03	1105.837898399	-0.04	4	50.00
9 mm	100	FMJ	1646	-9.14450233E-03	2.37736550E-03	-670.723217681	-3.09	1	0.00
9 mm	100[1]	JHP	1512	5.638407692003	2.76390508E-04	-3411.507895403	-2.44	5	20.00
9 mm	100	JSP	1519	-3.52531725E-03	2.74871185E-03	-684.0920454629	-1.33	1	0.00
9 mm	115	FMJ	1325	-2.44586917E-03	2.72627309E-03	-831.5696403531	-1.00	1	0.00
9 mm	115	JHP	1417	0.441116438577	2.86405759E-03	-797.6466613514	-3.92	5	20.00
38	90	Hemi/JSP	1250	-8.408132122255	6.60067664E-03	3681.056570682	0.00	3	33.33
38	110	JHP	1725	2.685827088166	1.48286991E-03	-1639.961723535	-1.84	11	27.27
38	125	JHP	1837	4.268997195447	8.61674999E-04	-2512.299353429	-3.65	13	30.76
38	148	WC	1794	1.260402154507	1.52503957E-03	186.5770158893	-4.79	1	0.00
38	158	JHP	1748	5.463778587451	2.41878706E-04	-2826.097748446	-2.23	11	45.45
38	158	JSP	1761	2.284496287811	1.79523251E-03	-1626.224818408	-0.62	7	42.85
38	158	LRN	1266	-5.033894694484	2.26967465E-03	1916.501103882	-2.55	1	0.00
38	158	SWC	1719	6.729291308774	-7.33217328E-05	-3918.064161714	-4.97	1	0.00

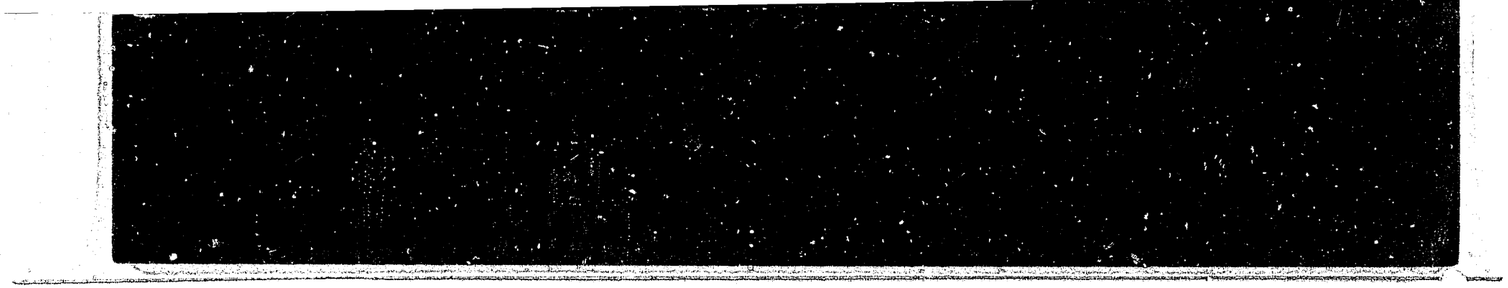

TABLE B7. *Speer*

Caliber	Weight (grains)	Type	Maximum test velocity (feet/second)	A	B	C	Average deviation	PTS	% pos.
9 mm	100	JHP	1512	5.638407692003	2.76390508E-04	-3411.507895403	2.71	6	66.66
9 mm	125	RN	1371	-5.36144609E-03	2.71962101E-03	-616.291409314	-2.10	1	0.00
9 mm	125	JSP	1351	-22.16397211567	1.34179180E-02	10851.68361002	0.23	6	33.33
38	110	JHP	1725	2.685827088166	1.48286991E-03	-1639.961723535	3.71	12	75.00
38	125	JHP	1837	4.268997195447	8.61674999E-04	-2512.299363429	7.94	6	100.00
38	125	JSP	1407	3.833194355271	9.99823834E-04	-2303.088990996	4.82	6	83.33
38	140	JHP	1512	8.473826178012	-1.05642851E-03	-4214.57575316	0.06	6	66.66
38	146	JHP	1318	-1.27993606E-02	3.01676941E-03	-242.5007425015	1.16	6	50.00
38	148	WC	1794	1.260402154507	1.52503957E-03	186.5770158893	0.01	11	36.36
38	158	JSP	1761	2.284496287811	1.79523251E-03	-1626.224818408	3.73	9	55.55
38	158	SWC	1719	6.729291308774	-7.33217328E-05	-3918.064161714	3.98	6	66.66
38	160	JSP	1450	25.59896790883	-6.63143142E-03	-17340.74304517	0.14	6	66.66
41	200	JHP	1368	-2.629323038823	3.22958938E-03	2939.900797912	0.27	6	33.33
41	220	JSP	1295	-15.27478457398	1.03597923E-02	7497.572173207	0.14	5	40.00
44	200	JHP	1240	3.666153538256	1.69946042E-03	-2163.581009684	4.37	5	100.00
44	225	JHP	1181	-1.31463143E-02	3.94006022E-03	-771.1731238753	-0.67	6	50.00
44	240	JSP	1302	-3.986962375353	5.12413614E-03	2044.717604744	0.72	12	33.33
44	240	SWC	1348	16.95871495063	-4.72439460E-03	-9532.682252896	1.04	6	50.00
45	200	JHP	1509	5.877362611534	2.93918304E-04	-2701.609584763	0.05	5	40.00
45	200	SWC	1489	-4.37863520E-03	2.41496855E-03	87.48117692936	-0.38	3	66.66
45	225	JHP	1387	5.374178693116	4.83344163E-04	-2527.46017364	0.98	4	50.00
45	250	SWC	1384	-2.14004939E-03	3.26195589E-03	-421.5422803956	-0.03	3	33.33

TABLE B8. *Supervel*

Caliber	Weight (grains)	Type	Maximum test velocity (feet/second)	A	B	C	Average deviation	PTS	% pos.
38	110	JHP	1725	2.685827088166	1.48286991E-03	-1639.961723535	5.47	6	50.00
38	110	JSP	1230	2.760793982647	1.49707574E-03	-1931.716267668	0.01	6	66.66
44	180	JSP	1601	-6.83223051E-03	2.45934328E-03	-126.370270803	-2.53	1	0.00

TABLE B9. *Winchester-Western*

Caliber	Weight (grains)	Type	Maximum test velocity (feet/second)	A	B	C	Average deviation	PTS	% pos.
9 mm	85	JHP	1226	10.71472550635	-3.27123883E-03	-4815.414726705	-0.01	5	40.00
9 mm	100	PP	1568	-3.084359160868	4.10145406E-03	1005.06277529	0.00	5	60.00
9 mm	115	PP	1371	-1.16236775E-02	2.17941083E-03	-359.9430776983	-2.53	1	0.00
9 mm	115	JHP	1504	25.8012946987	-8.62700386E-03	-14213.43479551	0.20	5	40.00
38	95	JHP	1418	15.45658126079	-4.50073683E-03	-8282.055408294	0.00	5	60.00
38	110	JHP	1725	2.685827088166	1.48286991E-03	-1639.961723535	0.72	19	68.42
38	148	WC	1794	1.260402154507	1.52503957E-03	186.5770158893	0.33	6	66.66
38	150	JSP	1289	-6.76358890E-04	2.98354213E-03	-592.1552588635	-0.49	1	0.00
38	150	LRN	1259	-13.17843674403	9.04175349E-03	6197.297802882	0.15	5	40.00
38	158	JHP	1748	5.463778587451	2.41878706E-04	-2826.097748446	3.48	20	60.00
38	158	JSP	1761	2.284496287811	1.79523251E-03	-1626.224818408	3.73	5	60.00
38	158	LHP	1312	4.858814531264	5.79790019E-04	-2353.228014494	0.50	13	61.53
38	158	LRN	1266	-5.033894694484	5.26967465E-03	1916.501103882	0.84	12	50.00
38	158	MP	1578	-2.11528401E-03	2.77168214E-03	-993.161798543	-9.31	2	50.00
38	158	SWC	1719	6.729291308774	-7.33217328E-05	-3918.064161714	2.95	4	75.00
45	185	FMJ	1272	-14.05354275485	7.85388481E-03	9026.046110245	0.00	3	66.66
45	185	JHP	1057	20.97949067896	-9.01010043E-03	-8676.315148547	0.00	5	60.00
45	230	FMJ	1164	-4.44360010E-03	2.77197163E-03	-536.5915478282	-1.12	2	50.00
45	255	LRN	1230	-8.73011535E-03	2.60455964E-03	-237.2871301171	-2.63	2	0.00

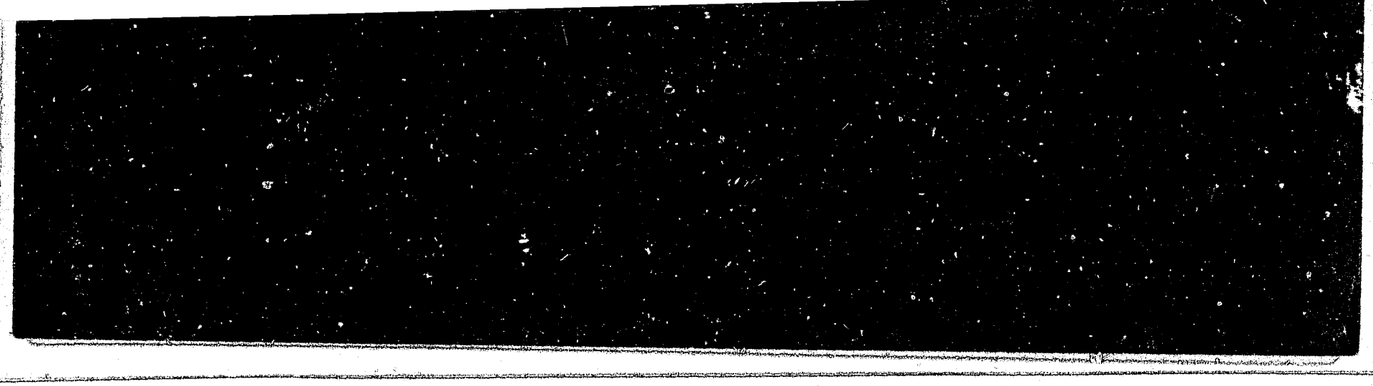

TABLE B10. *Zero*

Caliber	Weight (grains)	Type	Maximum test velocity (feet/second)	A	B	C	Average deviation	PTS	% pos.
38	100	JHP	1282	6.060524075061	-4.13052697E-04	-3010.963354593	0.07	5	60.00
38	110	JHP	1725	2.685827088166	1.48286991E-03	-1639.961723535	0.72	6	50.00
38	125	JHP	1837	4.268997195447	8.61674999E-04	-2512.299363429	-0.36	10	50.00

APPENDIX C—THEORETICAL CAVITY MODEL FOR NONDEFORMING PROJECTILES

Model Derivation

In a homogeneous medium such as ballistic gelatin the introduction of a kinetic energy projectile will cause stresses in the medium such as depicted in figure C1. Here the projectile is moving through the target medium along the Z-axis with instantaneous velocity V(Z). The dynamic pressure, P(Z), at the surface of the projectile can be represented by:

$$P(Z) = 1/2\ \rho_0\ C_D\ V^2\ (Z) + \sigma_0 \tag{C1}$$

where ρ_0 is the density of the target medium, C_D is the drag coefficient, and σ_0 is the flow stress of the target medium. The choice of the above equation is not unique but has been found to represent the "slow-down" of the bullet in the target with acceptable accuracy.

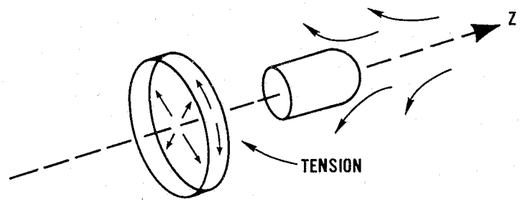

FIGURE C1. *Sketch of tissue response to bullet penetration.*

For the instance shown in figure C2, the dynamic pressure is interpreted to be the source for a stress wave propagating spherically outward from the point Z, the instantaneous position of the bullet. Consider an arbitrary observation point, Q. The local stress at Q, P_Q, due to the spherical wave originating at Z can be represented by:

$$P_Q = P(Z)\left[e^{-R/\lambda}\right]\left[1/R\right] \tag{C2}$$

The factor (1/R) is the geometric attenuation for the amplitude of a spherical wave, where R is defined in figure C2. The exponential factor is an empirical device to account for losses to the target medium. λ is an effective screening length and was determined for the gelatin material through data analysis. This screening length is characteristic of the distance the stress waves could propagate before being opposed by the medium.

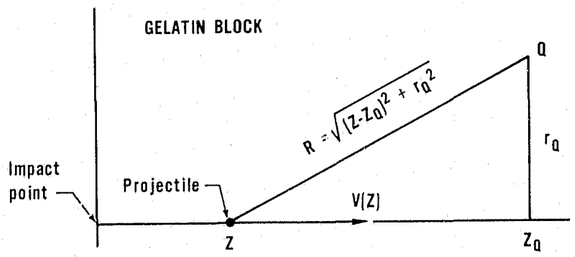

FIGURE C2. *Theoretical cavity model.*

The heuristic motivation for the model is based on the following:

$$\text{pressure} = \text{impulse flux} \tag{C3}$$

$$\text{force/area} = (\text{force} \cdot \text{time})\ (1/(\text{time} \cdot \text{area}))$$

From this relation we see that integrating an impulse flux over time is the same as integrating a pressure over time. Furthermore, if all of the impulse is delivered in a short time, one can approximate the total impulse per unit area by summing all of the pressure contributions which are present. In this way one can approximate what will be called the total "push" felt at Q with the following integral:

$$\left["\text{push}" \text{ at } Q\right] = \left[\frac{\text{impulse}}{\text{area}} \text{ at } Q\right] \cong \int_Q^{Z_Q} P(Z)\ \frac{\exp(-R/\lambda)}{R}\ dZ \equiv D\left(Z_Q, r_Q\right) \tag{C4}$$

In terms of the model geometry one sums all the contributions to the pressure at Q due to the dynamic pressure at the bullet from the time it enters the target until it passes by the observation point at Z_Q. This quantity is designated as $D(Z_Q, r_Q)$. Experimental evidence shows that very little displacement of the medium occurs until after the bullet passes by, thus supporting the assumption of a sudden impulse.

An important restriction on the applicability of the model is that the bullet must be moving slowly enough that the outgoing stress waves do not interfere with each other. This occurs when the bullet velocities are less than Mach 0.8 in the target medium. For gelatin, the speed of sound, Mach 1.0, is comparable to that in water; about 1450 m/s (4757 ft/s). Similarly, the speed of sound for fat tissue has been measured to be 1440 m/s (4724 ft/s) and for muscle to be 1570 m/s (5151 ft/s). Consequently, the model should only be applied to projectile velocities less than 1000 m/s (3281 ft/s).

The final step in the model is to postulate the existence of a critical value of $D(Z_Q, r_Q)$. This value, called D_c, is the impulse per unit area which delineates the temporary cavity envelope. This results in the following criteria for calculating the contour of the temporary cavity formed by bullet penetration:

1. If $D(Z_Q, r_Q) > D_c$, the point, Q, lies within the cavity envelope.
2. If $D(Z_Q, r_Q) < D_c$, the cavity will never advance as far as Q.
3. If $D(Z_Q, r_Q) = D_c$, then the point, Q, lies on the cavity boundary.

The cavity model is then of the form:

$$D_c = \int_0^{Z_Q} P(Z)\ \left[\frac{\exp(-R/\lambda)}{R}\right] dZ \tag{C5}$$

such that the MTC envelope is found by finding the locus of pairs of coordinates (Z_Q, r_Q) at which the above equation is satisfied.

From basic physics, pressure is measured as a force per unit area and force is given by mass times acceleration. These basic expressions can be combined as follows:

$$P(Z) = F/A = \frac{m\ \frac{d^2Z}{dz^2}}{A}$$

But

$$\frac{d^2Z}{dt^2} = \frac{dV}{dt} = \frac{dZ}{dt} \cdot \frac{dV}{dZ} = V\ \frac{dV}{dZ}$$

Where $V = \frac{dZ}{dt}$ remembering that in this case $\frac{dZ}{dt}$ is decreasing in value as time, t, increases.

Therefore:

$$-V\,dV = \frac{A}{m}P(Z)dZ \tag{C6}$$

Substituting eq (C1) into (C6) and rearranging yields:

$$-\frac{V\,dV}{\sigma_0+\frac{\rho_0 C_D V^2}{2}} = \frac{A}{m}dZ \tag{C7}$$

Equation (C7) can be integrated from the striking velocity, V_0, at a penetration distance, Z=0, to the velocity, V, at a penetration distance, Z.

$$-\int_{V_0}^{V}\frac{V\,dr}{\sigma_0+\frac{\rho_0 C_D V^2}{2}} = \int_0^Z \frac{A}{m}dZ$$

or

$$\int_{V_0}^{V}\frac{V\,dv}{\sigma_0+\frac{\rho_0 C_D V^2}{2}} = -\frac{A}{m}Z$$

from which

$$\frac{1}{\rho_0 C_D}\left[\ln\left(V^2+\frac{2\sigma_0}{\rho_0 C_D}\right)-\ln\left(V_0^2+\frac{2\sigma_0}{\rho_0 C_D}\right)\right] = -\frac{A}{m}Z$$

Raising both sides of the equation to the natural logarithm, base e, yields

$$\frac{V^2+\frac{2\sigma_0}{\rho_0 C_D}}{V_0^2+\frac{2\sigma_0}{\rho_0 C_D}} = \exp\left(-\frac{AZ}{\rho_0 C_D m}\right)$$

or

$$V^2(Z) = V_0^2\exp\left(-\rho_0 C_D\frac{AZ}{m}\right)+\frac{2\sigma_0}{\rho_0 C_D}\left[\exp\left(-\frac{\rho_0 C_D AZ}{m}\right)-1\right] \tag{C8}$$

Finally, substituting eq (C8) into (C1) and combining with (C5) model for the envelope of the MTC in gelatin due to the impact of a nondeforming kinetic energy projectile:

$$D_c = \int_0^{Z_Q}\frac{1}{2}\rho_0 C_D\left[V_0^2\exp\left(-\frac{\rho_0 C_D AZ}{m}\right)+\frac{2\sigma_0}{\rho_0 C_D}\left[\exp\left(-\frac{\rho_0 C_D AZ}{m}\right)-1\right]\right]\frac{\exp(-R/\lambda)}{R}\,dZ$$

where

$$R = \sqrt{(Z-Z_Q)^2+r_Q^2}$$

A is the presented area of the bullet and m is its mass. The values of C_D have been determined experimentally for bullets of different shape and are listed below in table C1. The values for the remaining parameters are as follows for gelatin:

$\rho_0 = 1.07\ g/cm^3$
$\sigma_0 = 2470\ dynes/cm^2$
$D_e = 1.4\times10^8\ dynes/cm^2$
$\lambda = 3.945\times\sqrt{A}\ cm$

TABLE C1. *Effective coefficients for typical bullet shapes assuming no deformation.*

C_D	Typical bullets
.3	Ball (full jacket), parabolic nose, power point
.37	Round nose, sphere, or hemi
.45	Semi-wadcutter, jacketed soft point
1.2	Wadcutter

Model Validation

For a theoretical or mathematical model to be useful, it must first be validated against existing data, then used to predict future data, and finally an experiment must be executed to verify that the model did predict the new data values with an acceptable accuracy. All three of these steps have been followed for the MTC model with one additional step. Due to the data that was available it was necessary to show first that gelatin and muscle performed similarly, and then that the model could be matched to the cavity formed in muscle tissue. Finally, the model was used to predict the performance of a real projectile in gelatin to complete the validation.

Figure C3 shows the contour of the MTC formed in gelatin and animal tissue for a 6.35 mm (.25 in) diameter sphere. The data points correspond to measurements of maximum radius of expansion as measured using a multiflash x-ray system. As seen in this figure, the gelatin data closely follows that for tissue. The differences are due to the fact that the tissue samples were not as thick as the gelatin samples.

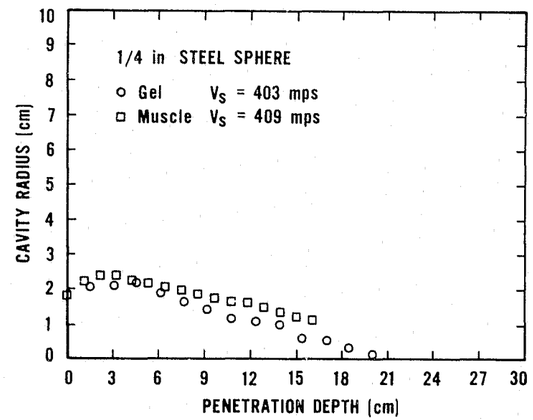

FIGURE C3. *Comparison of the maximum temporary cavity for a steel sphere penetrating animal tissue and tissue simulant.*

Following the above steps, figure C4 compares the MTC, formed in animal tissue and the cavity calculated by using the mathematical model with the appropriate values of ρ_0, λ, σ_0, and D_e for the animal tissue.

Finally, figure C5 compares the measured cavity in gelatin for a 38 caliber, 158 grain, jacketed soft point, bullet at a velocity of 372 m/s (1220 ft/s) with the cavity that the model would predict if the bullet does not deform. It can be seen that in this case the bullet cavity is larger than the model cavity over about the first 7.5 cm of penetration due to early bullet expansion. For the remainder of the penetration the bullet cavity was lower than the cavity computed for the nontumbling, nondeforming projectile. This reversal in cavity radius is due to the fact that the actual bullet was slowed down to a greater extent in the expansion stage and that after deformation the flat nose became somewhat rounded making the C_p lower. However, the model did satisfactorily predict the performance of the 38 caliber, 158 grain, projectile in the gelatin target. Depending on where the deformation occurs with respect to peaks in the vulnerability index curve, various changes in the RII's would be obtained.

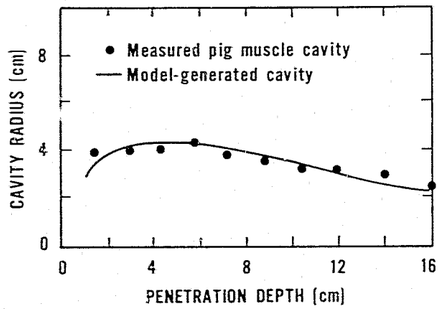

FIGURE C4. *Comparison of measured maximum temporary cavity (MTC) formed in animal tissue and a momentum transfer model prediction.*

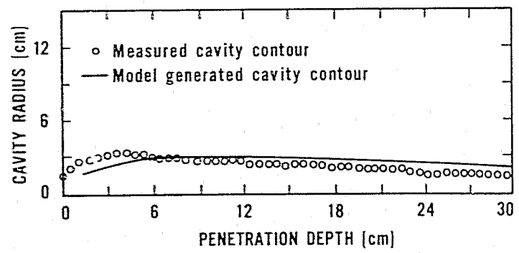

FIGURE C5. *Comparison of a measured cavity contour for a .357, 158 grain JSP bullet at 372 m/s velocity and model generated cavity contour for a similar nondeforming bullet.*

APPENDIX D—VULNERABILITY STUDIES

Once a method (computer model) of determining the vulnerability of a human body has been developed, it can be used to investigate the conditions that effect the probability that the handgun/shooter system will be effective. The section on the "Computer Man" discusses the manner in which the computer model develops the V. Ind. function. This appendix discusses the studies conducted using the model.

The first study concerns the effect of increased range to the target on target vulnerability. Figures D1, D2, and D3 show in graphical form the V. Ind. as a function of increasing target range for group A shooters. It is observed that as range increases both the amplitude and the area under the V. Ind. curve decrease indicating reduced vulnerability with increasing range.

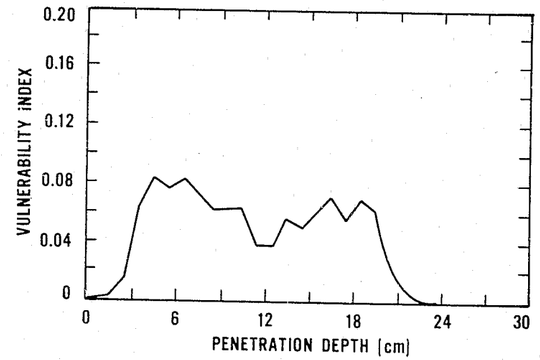

FIGURE D1. *Vulnerability index for handguns at a range of 3 m for the Group A hit distribution.*

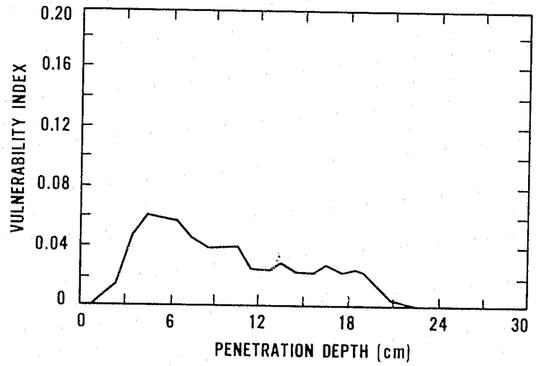

FIGURE D2. *Vulnerability index for handguns at a range of 6 m for the Group A hit distribution.*

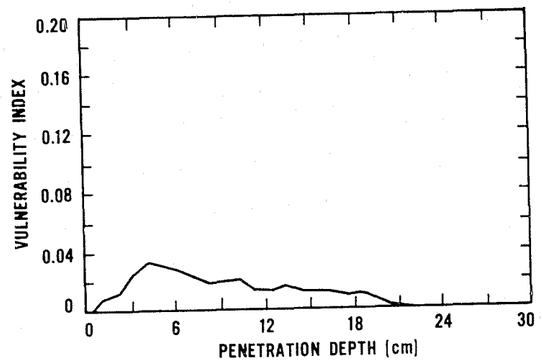

FIGURE D3. *Vulnerability index for handguns at a range of 12 m for the Group A hit distribution.*

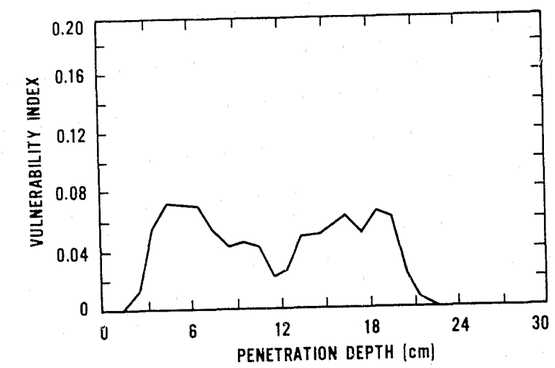

FIGURE D4. *Vulnerability index for handguns at a range of 6 m for the Group B hit distribution.*

Figure D4 depicts the V. Ind. for the Group B shooters at a target range of 6 m. Comparing figure D4 to figure D2 shows that increased shooter accuracy has a small effect on the maximum amplitude of the V. Ind. curve and a large effect on the area under the curve. Comparing figure D4 to D1, the curves are very similar. Obviously, increased shooter accuracy has the effect of providing bullet impacts at longer ranges similar to those at close range. These results are what one would expect, namely, increasing range decreases target vulnerability while increasing accuracy increases target vulnerability.

A more interesting study involves the choice of aim point. The aim point chosen for the V. Ind. used in the RII calculations in this report was the center of mass of the target, i.e., mid-thorax, and corresponds to the aim point on the standard silhouette target. However, the medical assessment showed that most of the vulnerable organs lie primarily in the upper half of the body. For the Group A hit distribution, many of the hits are on the lower half of the body which does not contain vulnerable organs. Figure 3 in the body of this report depicts this. The Group B distribution, on the other hand, is tight enough that many of the vulnerable organs that lie above the aim point are not hit. This implies that there may be an optimum aim point which lies higher than the generally accepted aim point.

Figure D5 illustrates the simulated impact points for a Group A hit distribution at a shooting range of 6 m with a mid-thorax, armpit high location as the desired impact point.

To determine if in fact the armpit high aim point is better, a vulnerability index was determined with the aim point shifted to approximately armpit level. It was found that the higher aim point concentrated the shots in an area where the vulnerable tissues lie closer to the front surface of the target. For this high aim point, it is expected that some of the rounds that do not penetrate as deeply as others and do not cause as much damage at greater depths of penetration for the low aim point would be more effective in terms of incapacitation.

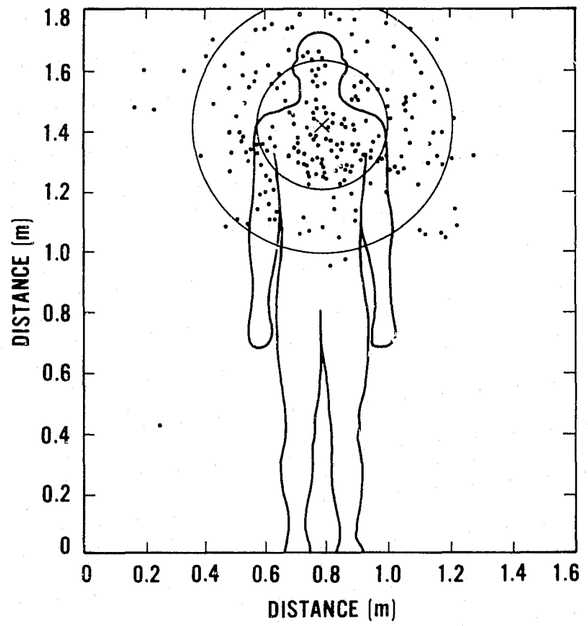

FIGURE D5. *High aim point hit distribution superimposed on a computer man silhouette for Group A shooters at a 6-m range.*

Figures D6 and D7 present the V. Ind. for Group A and Group B shooters respectively when the high aim point is used. When these two figures are compared to figure D2, it is clear by comparing both the amplitude and the area under the curve that the high aim point provides an increase in target vulnerability to incapacitation and that increased shooter accuracy combined with a high aim point dramatically increases the probability that an individual round will hit a tissue vulnerable to incapacitation.

In summary, for handguns used against human targets increasing range decreases the effective vulnerability of the target; however, increasing shooter accuracy can offset the effect of increased range. The use of an armpit high intended impact point increases the effective vulnerability of the target. Finally, the effect of increased shooter accuracy and the use of an armpit high aim point is to greatly increase the target's average vulnerability. It should be remembered that for the RII calculations performed in this report only the vulnerability index depicted as figure D2 (average trained shooters at 6 m) is used.

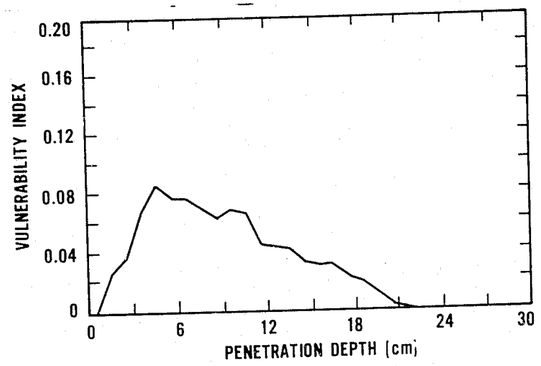

FIGURE D6. *Vulnerability index for handguns at a range of 6 m for the Group A hit distribution using a high aim point.*

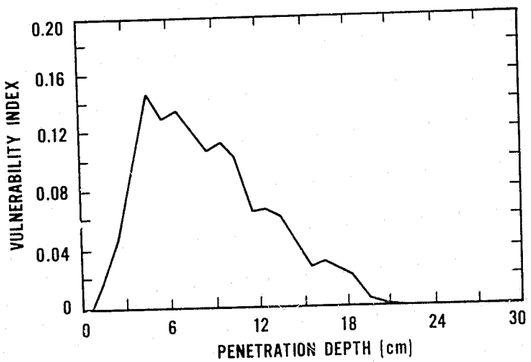

FIGURE D7. *Vulnerability index for handguns at a range of 6 m for Group B hit distribution using a high aim point.*

*U.S. GOVERNMENT PRINTING OFFICE : 1984 0-421-934/11202

END